CHEMISTRY
A EUROPEAN JOURNAL

DOI: 10.1002/chem.200601637

Possible Existence of Alkali Metal Orthocarbonates at High Pressure

Željko P. Čančarević, J. Christian Schön,* and Martin Jansen*[a]

Abstract: We investigate the possible existence of crystalline alkali metal orthocarbonates, A_4CO_4, where A = Li, Na, K, Rb, and Cs. We study the equilibrium between the possible modifications of the orthocarbonate A_4CO_4 and the binary mixture of the possible modifications of the alkali oxide A_2O and those of the alkali metal carbonate A_2CO_3 as function of pressure. In all cases, the orthocarbonate should be stable at sufficiently high pressure ranging from 22–32 GPa (Rb_4CO_4) to 200–220 GPa (Cs_4CO_4).

Keywords: alkali metal orthocarbonates · high pressure polymorphs · structure prediction

Introduction

Orthocarbonic acid is a tetraprotic acid and can be considered to be formed by the double hydration of carbon dioxide, which has not been observed thus far.[1] However, it has been shown computationally[2,3] that the most stable structure of H_4CO_4 corresponds to a local minimum on the energy landscape with an S_4 symmetry. Despite the absence of orthocarbonic acid and its salts, the orthocarbonate esters $(RO)_4C$ and $(ArO)_4C$ are well known.[1,3] The existence of these esters led to expectations that its salts, the orthocarbonates, should also be accessible.[4] Successful synthesis of the potassium, rubidium, and cesium trifluororthocarbonates $ACOF_3$ (A = K, Rb, Cs) by Ostwald ripening in CH_3CN applying a COF_2 pressure of 3 bar[5] support our idea that alkali metal orthocarbonates should also exist. Such compounds are of interest not only because they would fill a gap in the chemical systematics, but also because of the role they might play in the mineral forming processes in the Earth's crust and mantle at high pressure and temperature conditions.

Among the elements of the second Period, nitrogen is the only one that forms an "isolated" tetrahedral tetraoxo anion, the so-called orthonitrate.[6,7] All our attempts to synthesize alkali metal orthocarbonates from the corresponding carbonates and oxides in analogy to orthonitrates at ambient pressure have failed thus far. Nevertheless it appears to be a natural consequence of the pressure–coordination rule[8] that under high-pressure conditions The possibility exist to convert, for example, carbonate compounds into structures containing carbon in fourfold coordination by oxygen, since higher coordination usually results in smaller molar volume, which is favored at high pressure according to Le Chatelier's principle. This has led to predictions that at very high pressures the orthocarbonate Li_4CO_4 with isolated CO_4 units,[4]and a post-aragonite structure of $CaCO_3$ containing chains of CO_4 tetrahedra[9] might exist.

Since the synthesis route via the application of high hydrostatic pressures appears to be promising, we have started to investigate the relevant equilibria $A_2O + A_2CO_3 \rightleftarrows A_4CO_4$ (A = alkali metal) as a function of pressure using computational techniques. For this it is necessary to study the part of the enthalpy surface of the A/C/O system with composition A_4CO_4 at several different pressures, in order to determine as many candidates as possible for both ambient and high pressures. Of course, such an orthocarbonate would compete with high-pressure phases of the corresponding regular carbonates plus oxides which have previously been studied.[10,11]

As a consequence the orthocarbonate system poses an additional challenge because most work on structure prediction up to now has been restricted to chemical systems, where the competing phases correspond to different modifications of the same compound. However, for essentially all classes of ternary materials, an equilibrium exists between the ternary phase and the constituting binary phases, for a given overall composition. The range of (thermodynamic) stability of such a ternary phase is a function of applied tem-

[a] Dr. Ž. P. Čančarević, Priv. Doz. Dr. J. C. Schön, Prof. Dr. M. Jansen
Max-Planck-Institut für Festkörperforschung
Heisenbergstrasse 1, 70569 Stuttgart (Germany)
Fax: (+49) 711-689-1502
E-mail: c.schoen@fkf.mpg.de
m.jansen@fkf.mpg.de

Supporting information for this article is available on the WWW under http://www.chemeurj.org/ or from the author.

WILEY InterScience DISCOVER SOMETHING GREAT
© 2007 Wiley-VCH Verlag GmbH & Co. KGaA, Weinheim

perature and pressure. For instance, for a given overall composition, at standard pressure two binary phases might be observed, while in the high-pressure regime only one ternary compound of the prescribed composition exists.

The identification of stable phases of such systems in an efficient fashion[12,13] requires the exploration of the enthalpy landscapes of all relevant binary and ternary compounds in a given chemical system, together with a computation of the (free) enthalpy of various combinations of these compounds under the condition of constant overall composition. In earlier work, several structure candidates for Li_4CO_4 have been presented.[4] However, the crucial issue of the competition between the orthocarbonate and the 1:1 mixture of the alkali metal oxide A_2O and the alkali metal carbonate A_2CO_3 including both phases stable at ambient pressure and those stable at high pressures was not considered. As a first step towards addressing this issue, we have computed the pressure-phase diagrams of the alkali metal carbonates A_2CO_3[10] and the alkali metal oxides A_2O[11] (A = Li, Na, K, Rb, Cs).

In this work, we study the enthalpy landscapes of the alkali metal orthocarbonates A_4CO_4. For each of these systems, we determine the thermodynamically stable phase as a function of pressure, and compare the enthalpies of the orthocarbonates with those of the 1:1 mixture of the corresponding oxides and carbonates.

Methods

Modeling the landscape: Our general approach to the determination of structure candidates has been given in detail elsewhere.[12,14] A summary of the procedure is given here: The structure candidates that should be capable of existence, at least at low temperatures, correspond to local minima of the enthalpy hypersurface ($H = E_{pot} + pV$) of the chemical system under investigation. Finding these candidates requires the use of a global optimization method as well as local optimization procedures, since we permit free variation of atom positions, cell parameters, ionic charges and composition, during the global landscape exploration. Since global optimization methods, in general, involve many millions of energy evaluations for atomic configurations, one usually cannot perform the energy calculations using ab initio methods. Therefore, we modeled the systems as spherical ions that interact via a simple empirical two-body interaction potential, $V_{ij}(r_{ij})$, consisting of a Coulomb and a Lennard-Jones term that depend only on the atom–atom distance r_{ij} in order to allow fast calculations of the energy, $E_{pot} = \Sigma_{i<j} V_{ij}(r_{ij})$, of a given configuration:

$$V_{ij}(r_{ij}) = \frac{q_i q_j}{r_{ij}} \exp(-\mu r_{ij}) + \varepsilon_{ij}\left[\left(\frac{\sigma_{ij}}{r_{ij}}\right)^{12} - \left(\frac{\sigma_{ij}}{r_{ij}}\right)^{6}\right] \quad (1)$$

The parameters entering the empirical potential are the sum of the ionic radii multiplied by a scaling factor r_s, $\sigma_{ij} = r_s(r_{ion}(i) + r_{ion}(j))$, the parameters ε_{ij}, and the convergence parameter μ. The ionic radii of the metal cations employed during the landscape explorations in this work were taken from Emsley:[15] $r_{ion}(Li^+) = 0.78$ Å, $r_{ion}(Na^+) = 0.98$ Å, $r_{ion}(K^+) = 1.33$ Å, $r_{ion}(Rb^+) = 1.49$ Å, $r_{ion}(Cs^+) = 1.65$ Å. Furthermore, we used $r_s = 1.1$, $\varepsilon_{ij} = 0.4$ and $\mu = 0.1$.

Since we are only interested in those modifications in the A/C/O system, which consist of metal cations and CO_4-complex anions, we employed fixed $(CO_4)^{4-}$ building units during the global optimizations. The building unit was treated as rigid with fixed charge distribution for each individual optimization run, and we used two limiting charge distributions, ($q(C) = +4$, $q(O) = -2$) and ($q(C) = 0$, $q(O) = -1$), and a tetrahedral shape analogous to SiO_4 units in crystobalite.

Since this structural unit has not yet been observed within an extended solid, we have previously optimized the size of the building units over a range of C–O distances, that is, d(C-O) = 1.37–1.57 Å, using a feedback loop between the global and local optimization stages.[4] The lower limit of d(C–O) was chosen to approximate the sum of the ionic radii of C^{4+} and O^{2-}, while the upper limit was based on the repulsion between the oxygen ions analogous to the one in the SiO_4 tetrahedron in crystobalite. During the global optimization stage of the feedback loop, the building unit was treated as a rigid soft body with fixed charge distribution for each individual optimization run. The adjustment of the size of the building unit occurred by alternating empirical-potential global optimizations and ab initio level local optimizations for the structure candidates found in the global optimization step. The final C–O distance of d(C–O) = 1.42 Å is in satisfactory agreement with those experimentally determined for molecules containing a COF_3 unit.[5]

Since we are interested in crystalline compounds, we have introduced periodic boundary conditions and employed up to three formula units during the global optimizations. The calculations were repeated for a number of pressures starting with a pressure of one atmosphere increasing in steps by a factor of 10 up to 1 TPa, and similarly for negative pressures up to −100 GPa. The negative pressure range is of interest for several reasons: In many cases modifications found to be deep-lying local minima at negative pressures happen to be thermodynamically preferred phases at high temperatures at standard pressure, reminiscent of Ostwald's rule.[16] Similarly, such a modification found at negative pressures can occur as a low-temperature modification at standard pressure in one of the homologue systems.[8] Finally, such modifications can occur if the synthesis takes place under effective negative pressures, for example, crystal growth within a low-density amorphous matrix.[17]

Optimization procedures and selection of basis sets: The global optimizations were performed by employing the stochastic simulated annealing algorithm,[18,19] with a temperature schedule $T_n = T_0\gamma^n$ ($\gamma = 0.95, \ldots, 0.995$). The moveclass consisted of atom movement and building unit rotation (about 80% of the moves), atom exchange (5%), and random variations of the cell parameters (15%), keeping

 © 2007 Wiley-VCH Verlag GmbH & Co. KGaA, Weinheim

the ionic charges fixed. In order to determine which combination of basis sets is optimal for the ab initio calculations, a number of basis sets were tested for A_2O, A_2CO_3 and A_4CO_4. Some of the basis sets were all-electron basis sets[20] (AEBS),[1] and some were "Stuttgart/Cologne-type" pseudopotential basis sets[21] (PPBS), in the case of Rb (ECP28MWB), and Cs (ECP46MWB). The optimal outermost shell exponents were optimized through energy minimization of the crystal energy. The final optimized basis sets can be found in references [10] and [11].

Weighting of phase contributions and determination of transition pressures: In addition to the optimized cell parameters, the $E(V)$ curves found by the local optimizations in a given chemical system X (X = A_2O, A_2CO_3 or A_4CO_4) yield the bulk modulus B_0 by fitting the calculated data points to the Murnaghan equation:[22]

$$E(V) = \frac{VB_0}{B_0'}\left[\frac{(V_0/V)B_0'}{B_0'-1}+1\right]-C \qquad (2)$$

where the four fit parameters B_0 and B_0' are the bulk modulus and its derivative, V_0 the equilibrium volume, and C the zero of the energy scale. By calculating the enthalpies:

$$H_i = E_i(V) + pV = E_i(V) - \frac{\partial E}{\partial V}V \qquad (3)$$

for the various structure candidates i, we determine the transition pressures between different modifications i and j by setting the enthalpies equal, $H_i = H_j$.

For a given pressure p, the minimum of the enthalpies $H_i^X(p)$ over all modifications i found in the system X yields the enthalpy of system X as function of pressure $H^X(p)$. By comparing the appropriately weighted average of $H^{A_2O}(p)$ and $H^{A_2CO_3}(p)$ with $H^{A_4CO_4}(p)$, $H_{comb}(p) = H^{A_2O}(p) + H^{A_2CO_3}(p)$, we can then calculate the pressure range, where the orthocarbonate is stable against disproportionation into the corresponding oxide and the carbonate.

In practice, we first compute the combined $E(V)$ curve of the A_2O-plus-A_2CO_3 system, $E_{comb}(V)$, via an inverse Legendre transform of $H_{comb}(p) = H^{A_2O}(p) + H^{A_2CO_3}(p)$. Since we have generated the enthalpies $H^{A_2O}(p)$ and $H^{A_2CO_3}(p)$ via Equation (3), the simple geometric construction shown in Figure 1 can be employed to generate $E_{comb}(V)$ from $H_{comb}(p)$. We note that $V = V^{A_2O}(p) + V^{A_2CO_3}(p)$, where $V^{A_2O}(p)$ and $V^{A_2CO_3}(p)$ are the volumes, at which the slope of $\partial E/\partial V$ equals $(-p)$. The same relation must hold true for $E_{comb}(V)$, which implies that $E_{comb}(V)$ is the curve given by the set of all points $(V, E_{comb}(V))$, where $V = V^{A_2O}(p) + V^{A_2CO_3}(p)$, and

[1] [1]Li (6-1G), Na (8-511G*), K (86-511G*), C (6-21G*) and O (8-411G)

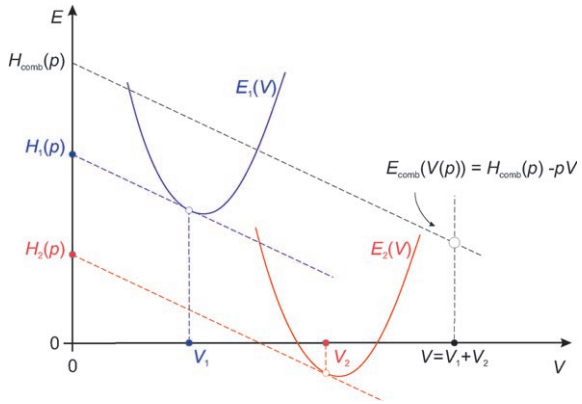

Figure 1. Construction of the point $E_{comb}(V(p))$ of the $E(V)$ curve representing the mixture of 1 and 2 at a given pressure $p = -\frac{\partial E_1}{\partial V} - \frac{\partial E_2}{\partial V} = \frac{\partial E_{comb}}{\partial V}$ starting from the $E(V)$ curves for the individual components and using Equation (3). The complete curve $E_{comb}(V)$ is constructed by repeating this procedure for all pressures, and is given by the envelope of the line $H_{comb}(p) - pV$.

$$\begin{aligned} E_{comb}(V) &= H_{comb}(p) - pV \\ &= H^{A_2O}(p) + H^{A_2CO_3}(p) - p(V^{A_2O}(p) + V^{A_2CO_3}(p)) \\ &= E^{A_2O}(p)(V^{A_2O}(p)) + E^{A_2CO_3}(V^{A_2O}(p)) \end{aligned} \qquad (4)$$

Note that if we had only access to $H_{comb}(p)$, we would have computed $V(p)$ via $V = \partial H_{comb}/\partial p$, that is:

$$E_{comb}(V) = H_{comb}(p) - p\frac{\partial H_{comb}}{\partial p} \qquad (5)$$

Using $E_{comb}(V)$ and the $E(V)$ curves of the hypothetical modifications of A_4CO_4, $E_i(V)$, we then compute the transition pressures by determining the common tangent between $E_{comb}(V)$ and $E_i(V)$.

Results

Results of the global search: After performing more than 2500 global optimizations with Z formula units per simulation cell ($Z = 1, 2, 3$), 262 structures with space groups other than $P1$ or $P\bar{1}$ were observed. After elimination of duplicates, eighty seven different new structure types were found to constitute local minima on the various enthalpy landscapes. After a preliminary ranking of the structures on ab initio level, we have reduced the list of the most promising structure candidates to 52. A list of the new structure types after local optimizations employing the Hartree–Fock method is given in Tables 1–5; for DFT-B3LYP data, see Supporting Information: Tables S1.1–1.5).

The overview in Figure 2 shows that on average for each pressure, up to 45% of the optimization runs resulted in structures with space groups other than $P1$ or $P\bar{1}$. The number of formula units applied in the simulation appears to have an influence on the diversity of the structure candidates, ranging from essentially 100% $P1$ or $P\bar{1}$ structures for

 © 2007 Wiley-VCH Verlag GmbH & Co. KGaA, Weinheim

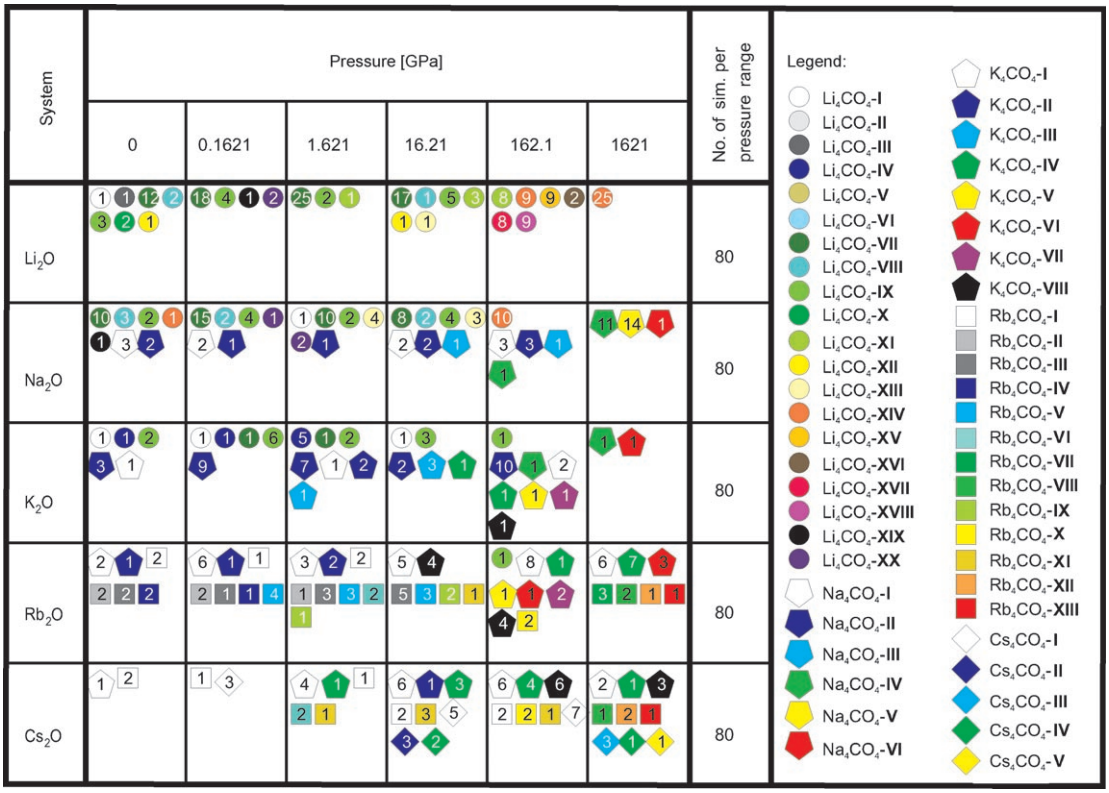

Figure 2. Distribution of the structure candidates over different pressure ranges for the A_4CO_4 system (A = Li, Na, K, Rb, and Cs). Structures with space group $P1$ or $P\bar{1}$ are not listed in order to avoid overloading the figure. In each entry, the different structure types are listed that were observed during the global optimization on the enthalpy landscape in the particular system at the specific pressure. Each structure type is represented by a symbol, and the number inside the symbol shows the number of times this particular local minimum had been found.

three formula units (in all systems) to about 35% for one formula unit in the case of Li_4CO_4. The number of different structure types (besides those with space group $P1$ or $P\bar{1}$) summed over all pressures for a given system ranged from 15 for Na_4CO_4, over 16 for Rb_4CO_4, 18 for Li_4CO_4, to 19 for both K_4CO_4 and Cs_4CO_4. In all systems, the number of different structure candidates shows a clear peak at the high end of the intermediary pressure range, and this peak is shifted to somewhat higher pressures with increasing cation size.

Regarding the kinetic stability of these structures, we have no quantitative data, since no threshold runs[23,24] have been performed for this system. However, some of the structures were found during global optimizations over a rather wide range of pressures, indicating that they should possess a rather high degree of stability as long as the CO_4 unit itself remains stable. In our earlier work,[4] we have also performed global optimizations for a wide range of pressures in the Li_4CO_4 system employing carbon and oxygen atoms/ions instead of a CO_4 unit together with lithium atoms/ions. These explorations have shown that for high pressures the coordination of carbon by oxygen changes from three (trigonally planar) to four (tetrahedral), suggesting that at sufficiently high pressures, the fourfold coordination will be stable.

Results of the local optimizations: In each system, the local refinement optimizations were performed for the most promising new candidates found during the global optimizations in the A_4CO_4 system. The resulting $E(V)$ curves, when using the HF approximation, are given in Figures 3, 5, 7, 9 and 11; the analogous curves for the DFT calculations are very similar (see Supporting Information Figures S1.1–S1.5 and Tables S1.1–S1.5). The optimized cell parameters and bulk moduli found employing the HF approximation for the selected structure candidates are given in Tables 1–5.

By comparing $H^{A_4CO_4}(p)$ with the appropriately weighted average of $H^{A_2O}(p)$ and $H^{A_2CO_3}(p)$, $H_{comb}(p) = H^{A_2O}(p) + H^{A_2CO_3}(p)$, the pressure ranges where the orthocarbonate is stable against disproportionation into the corresponding oxide and the carbonate have been calculated. We find that in all systems the combined $E(V)$ curve of the A_2O-plus-A_2CO_3 system at standard pressure corresponds to the thermodynamically stable structure, while at high pressures some modification of A_4CO_4 should be favored. These results agree with the experimental observation that these hypothetical modifications do not appear to be thermodynamically stable at low pressures.

Unexpectedly, potassium and rubidium show relatively low transition pressures from A_2O-plus-A_2CO_3 to the hypothetical modifications of the A_4CO_4 system. This contradicts

 © 2007 Wiley-VCH Verlag GmbH & Co. KGaA, Weinheim

the usual "chemical intuition", since if one considers the cation size to be the crucial quantity, one would expect Li_4CO_4 to have the lowest transition pressure. On the other hand, the cesium cation's basicity tends to favor a more localized type of bond, leading to the alternative expectation that Cs_4CO_4 should be the first orthocarbonate to be found with increasing pressure.

One should note that several interesting hypothetical high-pressure modifications fit into a scheme suggested by Nuss[25] in the system A_4TiX_4, where he treats the A_4TiX_4 unit as a neutral heterocubane. The heterocubane is the tetrahedral structural derivative of the simple cube, and even rock salt can be described as a simple cubic packing of "Na_4Cl_4 heterocubanes".[26] Since the orthocarbonates are rather complicated structures to plot and interpret from a chemical point of view we have attempted to describe our structures as 3D arrangements of heterocubanes when appropriate. The structures are shown below (see Figure 14–20).

Results restricted to Li_4CO_4: The mixture of Li_2O and Li_2CO_3 is stable over a wide range of pressure up to about 80–110 GPa. A mixture between the $CaCl_2$-type (Li_2O system) and γ-Cs_2CO_3 (Li_2CO_3 system) exists in the range of high effective negative pressures. Then we observe a collapse of volume due to a transition of the carbonate from the γ-Cs_2CO_3 to the Li_2CO_3-type-19 modification at moderate negative pressures. One should note that those pressures have only a meaning from a calculation point of view, since even when growing a crystalline phase inside a low-density amorphous matrix[17] experimentally only effective negative pressures of at most a few GPa can be reached. At about −10 GPa, a transition for the oxide takes place: the $CaCl_2$ structure type undergoes a phase transition to the fluorite structure type (CaF_2-type). From approximately −5 GPa up to 10 GPa there exists a mixture of the CaF_2-type, for the oxide and the Zabujelite structure type for the carbonate. This is followed by a phase transition to the HP-Li_2CO_3-type structure in the carbonate. Finally, the CaF_2-type should undergo a pressure induced phase transition to the γ-US_2 structure (for more details see refs. [10,11]).

From Figures 3 and 4 and Table 1 (for DFT-B3LYP data see Supporting Information Figure S1.1 and Table S1.1), we see that in the Li_4CO_4 system it should be possible to synthesize orthocarbonates for pressures between 80–110 GPa. According to our calculations a phase transition should occur from a mixture of the γ-US_2-type modification of Li_2O and the HP–Li_2CO_3 phase for Li_2CO_3 to the Li_4CO_4-**X** in the Li_4CO_4 system. As we discussed in earlier work,[27] one would expected from general considerations, that the Hartree–Fock calculations produce larger equilibrium volumes and higher transitions pressures than the DFT ones, with the experimental values lying somewhere in-between. The predicted transition pressure is rather high and is most likely the reason why all attempts to synthesize Li_4CO_4 in the range of pressures up to 50 GPa[28] have failed thus far. The possible high-pressure structures in the Li_4CO_4 system are shown below (see Figure 14). According to nomenclature introduced in references [25] and [26], the structure Li_4CO_4-**X** belongs to the *tI*2(*I*) arrangement of heterocubanes. Table 1 and Table S1.1 in the Supporting Information show structural data, minimum volumes, bulk moduli and energies of selected structure candidates for the Li_4CO_4 system after local optimizations on Hartree–Fock and DFT-B3LYP basis, respectively.

Results restricted to Na_4CO_4: Similar to the Li_4CO_4 system, the most promising structure candidates found for Na_4CO_4 were chosen for refinement optimizations. The $E(V)$ curves were computed and are shown in Figure 5 and Table 2 (for DFT-B3LYP data see Supporting Information Figure S1.3 and Table S1.2). The transition to the orthocarbonates should occur at 37–60 GPa (cf. Figure 6). In the case of the Na_4CO_4 system we have observed a number of phase transitions. As we can see in Figure 5, in the range of very high

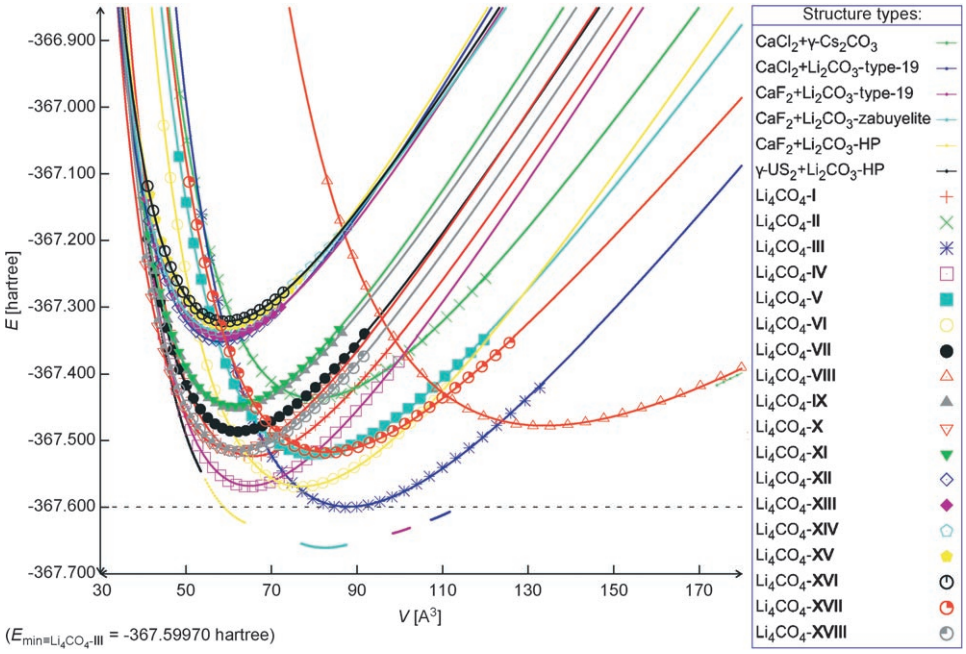

Figure 3. $E(V)$ curves for selected structure candidates calculated on ab initio level (HF) in the Li_4CO_4 system together with the combined curve for $Li_2O+Li_2CO_3$. The dashed horizontal line refers to the energy minimum of the Li_4CO_4 system (E_{min}).

 © 2007 Wiley-VCH Verlag GmbH & Co. KGaA, Weinheim

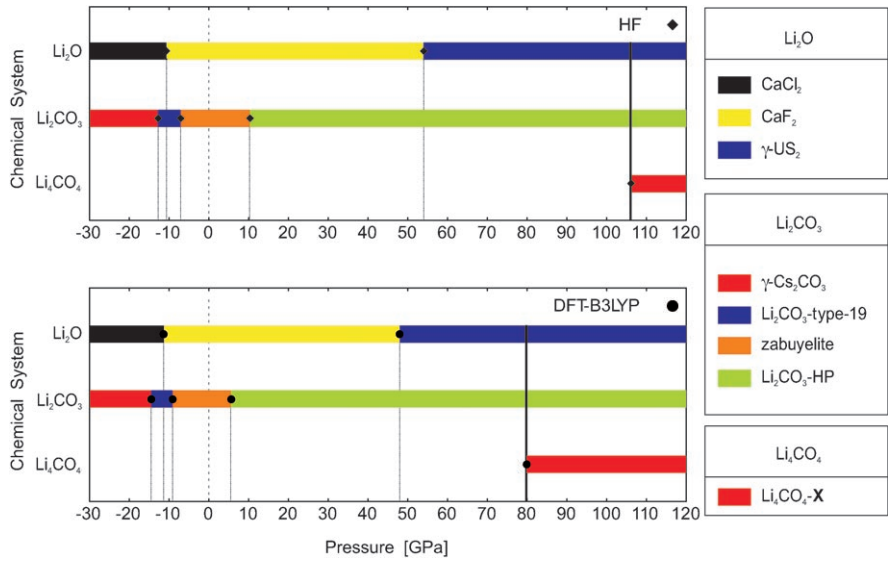

Figure 4. Low-temperature modifications of Li_4CO_4 as function of pressure in equilibrium with the solid state reaction $Li_2O + Li_2CO_3$. Only the modifications with the lowest enthalpy are depicted. Upper box: HF. Lower box: DFT-B3LYP.

negative pressures a $CaCl_2$ oxide modification exists together with γ-Cs_2CO_3 (green line), and then a β-Rb_2CO_3 (blue line) and α-Na_2CO_3 (magenta line) carbonate modification. The next phase transition for the oxide is from the $CaCl_2$- to the CaF_2-structure type. Short cyan and yellow lines show the transition between the α-Na_2CO_3- and the β-Na_2CO_3-carbonate modification with the oxide in the CaF_2-structure type. In the range of pressures between −5 GPa to 5 GPa (about 10 GPa according to HF calculations) we find the oxide CaF_2- and the carbonate γ-Na_2CO_3 modification. Upon increasing pressure, several phase

Table 1. Data for structure candidates for Li_4CO_4 after local optimizations on ab initio level (HF).

Space group (no.) crystal system, type	Lattice constants (a,b,c [Å]; α,β,γ [°])	Atom (multiplicity, Wyckoff letter), relative coordinates				V_{min} [Å^3]	E_{min} [a.u.]
		atom	x	y	z		
$P\bar{4}3m$ (215)	a=4.03079	C1(1b)	0.5	0.5	0.5	65.489	−367.5238
cubic	$\alpha=\beta=\gamma$=90	O1(4e)	0.29764	0.29764	0.29764	164.017	
Li_4CO_4-**I**		Li1(4e)	0.78515	0.78515	0.78515		
$R3m$ (160)	a=4.32623	C1(1a)	0.99961	0.99961	0.99961	80.020	−367.4370
trigonal	$\alpha=\beta=\gamma$=84.77741	O1(3b)	0.81909	0.19316	0.81909	142.917	
Li_4CO_4-**II**		O2(1a)	0.16322	0.16322	0.16322		
		Li1(1a)	0.71409	0.71409	0.71409		
		Li2(3b)	0.49861	0.10286	0.49861		
$I\bar{4}2m$ (121)	a=6.39767	C1(2b)	0	0	0.5	175.659	−367.5997
tetragonal	c=4.29166	O1(8i)	0.12253	0.12253	0.30592	126.680	
Li_4CO_4-**III**	$\alpha=\beta=\gamma$=90	Li1(8i)	0.82438	0.82438	0.85875		
$I\bar{4}2m$ (121)	a=4.04978	C1(2a)	0	0	0	129.690	−367.5686
tetragonal	c=7.90755	O1(8i)	0.79583	0.79583	0.90050	167.560	
Li_4CO_4-**IV**	$\alpha=\beta=\gamma$=90	Li1(8i)	0.69676	0.69676	0.14250		
Cm (8)	a=6.55195	C1(2a)	0.00348	0	0.49870	159.491	−367.5201
monoclinic	b=6.33513	O1(4b)	0.00048	0.81681	0.69332	137.759	
Li_4CO_4-**V**	c=3.85795	O2(2a)	0.81207	0	0.24347		
	$\alpha=\gamma$=90	O3(2a)	0.18915	0	0.35486		
	β=95.13547	Li1(4b)	0.31427	0.21696	0.00993		
		Li2(4b)	0.20302	0.70794	0.47902		
$C2$ (5)	a=8.09241	C1(2a)	0	0.22106	0	153.522	−367.5692
monoclinic	b=4.46021	O1(4c)	0.87897	0.04668	0.08557	148.057	
Li_4CO_4-**VI**	c=4.39575	O2(4c)	0.08652	0.41015	0.25390		
	$\alpha=\gamma$=90	Li1(4c)	0.31673	0.60461	0.44660		
	β=104.62042	Li2(4c)	0.13494	0.63680	0.90308		
Cm (8)	a=5.30896	C1(2a)	0.47214	0	0.55192	124.980	−367.4861
monoclinic	b=5.98005	O1(2a)	0.30191	0	0.73538	166.404	
Li_4CO_4-**VII**	c=4.43162	O2(4b)	0.40212	0.19977	0.33911		
	$\alpha=\gamma$=90	O3(2a)	0.77490	0	0.79577		
	β=117.33880	Li1(2a)	0.67213	0	0.28867		
		Li2(2a)	0.07626	0	0.25643		
		Li3(4b)	0.56275	0.72981	0.81968		
$C2$ (5)	a=9.11258	C1(2b)	0	0.60555	0.5	267.186	−367.4780
monoclinic	b=3.91271	O1(4c)	0.48856	0.31775	0.65616	73.878	
Li_4CO_4-**VIII**	c=7.50333	O2(4c)	0.37139	0.89447	0.47686		
	$\alpha=\gamma$=90	Li1(4c)	0.48814	0.82740	0.69961		
	β=92.90730	Li2(4c)	0.33740	0.38760	0.47157		

© 2007 Wiley-VCH Verlag GmbH & Co. KGaA, Weinheim

Table 1. (Continued)

Space group (no.) crystal system, type	Lattice constants (a,b,c [Å]; α,β,γ [°])	Atom (multiplicity, Wyckoff letter), relative coordinates				V_{min} [Å^3]	E_{min} [a.u.]
		atom	x	y	z		
*R*3*m* (160)	$a=3.99573$	C1(1a)	0.51019	0.51019	0.51019	61.642	−367.4516
trigonal	$\alpha=\beta=\gamma=98.17150$	O1(3b)	0.29134	0.29134	0.68906	166.885	
Li_4CO_4-**IX**		O2(1a)	0.76449	0.76449	0.76449		
		Li1(3b)	0.78601	0.78601	0.27705		
		Li2(1a)	0.18787	0.18787	0.18787		
*C*2 (5)	$a=8.42360$	C1(2a)	0	0.81063	0	121.953	−367.5144
monoclinic	$b=3.90118$	O1(4c)	0.39064	0.09003	0.69800	170.893	
Li_4CO_4-**X**	$c=4.06293$	O2(4c)	0.61150	0.52998	0.88541		
	$\alpha=\gamma=90$	Li1(4c)	0.63308	0.58821	0.41584		
	$\beta=114.02130$	Li2(4c)	0.63721	0.03126	0.83017		
Cm (8)	$a=5.23401$	C1(2a)	0.99962	0	0.60672	122.619	−367.4469
monoclinic	$b=5.97460$	O1(4b)	0.51033	0.29793	0.38925	170.300	
Li_4CO_4-**XI**	$c=3.95016$	O2(2a)	0.75346	0	0.75886		
	$\alpha=\gamma=90$	O3(2a)	0.21916	0	0.88522		
	$\beta=96.94540$	Li1(2a)	0.31680	0	0.40552		
		Li2(4b)	0.43371	0.24098	0.87994		
		Li3(2a)	0.72041	0	0.26351		
Cm (8)	$a=5.06964$	C1(2a)	0.91363	0	0.48026	116.350	−367.3515
monoclinic	$b=6.10094$	O1(4b)	0.46599	0.70937	0.71905	179.714	
Li_4CO_4-**XII**	$c=3.95496$	O2(2a)	0.11847	0	0.25718		
	$\alpha=\gamma=90$	O3(2a)	0.61036	0	0.22877		
	$\beta=107.98160$	Li1(2a)	0.28361	0	0.79255		
		Li2(4b)	0.33729	0.25108	0.69167		
		Li3(2a)	0.66545	0	0.74117		
Cm (8)	$a=5.54844$	C1(2a)	0.68497	0	0.41084	117.630	−367.3442
monoclinic	$b=5.67002$	O1(4b)	0.23723	0.27556	0.64950	173.609	
Li_4CO_4-**XIII**	$c=4.04379$	O2(2a)	0.39552	0	0.14848		
	$\alpha=\gamma=90$	O3(2a)	0.86510	0	0.19789		
	$\beta=112.38560$	Li1(4b)	0.10967	0.76843	0.10759		
		Li2(2a)	0.47684	0	0.69234		
		Li3(2a)	0.03061	0	0.72036		
*Pmn*2$_1$ (31)	$a=5.99085$	C1(2a)	0	0.31488	0.33828	115.807	−367.3365
orthorhombic	$b=4.01834$	O1(2a)	0	0.62994	0.15139	176.800	
Li_4CO_4-**XIV**	$c=4.81059$	O2(4b)	0.78894	0.10490	0.27753		
	$\alpha=\beta=\gamma=90$	O3(2a)	0	0.42196	0.64743		
		Li1(2a)	0	0.07319	0.95632		
		Li2(4b)	0.74533	0.59738	0.42713		
		Li3(2a)	0	0.91688	0.55454		
Pc (7)	$a=4.24568$	C1(2a)	0.15995	0.22280	0.28843	118.647	−367.3289
monoclinic	$b=5.68262$	O1(2a)	0.20064	0.95623	0.33259	181.629	
Li_4CO_4-**XV**	$c=5.76918$	O2(2a)	0.49622	0.31868	0.28930		
	$\alpha=\gamma=90$	O3(2a)	0.12975	0.33589	0.51644		
	$\beta=121.52540$	O4(2a)	0.81216	0.27487	0.01175		
		Li1(2a)	0.79382	0.55401	0.195280		
		Li2(2a)	0.58377	0.13209	0.63821		
		Li3(2a)	0.83940	0.05177	0.43795		
		Li4(2a)	0.30856	0.60528	0.39874		
*Cmc*2$_1$ (36)	$a=5.83423$	C1(4a)	0	0.34269	0.35112	237.101	−367.3216
orthorhombic	$b=7.83887$	O1(8b)	0.71592	0.95173	0.29390	170.137	
Li_4CO_4-**XVI**	$c=5.18436$	O2(4a)	0	0.18282	0.17372		
	$\alpha=\beta=\gamma=90$	O3(4a)	0	0.28758	0.63842		
		Li1(8b)	0.73916	0.20876	0.42484		
		Li2(4a)	0	0.43034	0.01613		
		Li3(4a)	0	0.96461	0.99771		
*C*2 (5)	$a=9.18281$	C1(2b)	0	0.04704	0.5	165.671	−367.5180
monoclinic	$b=3.88289$	O1(4c)	0.86458	0.83189	0.24796	123.088	
Li_4CO_4-**XVII**	$c=6.23464$	O2(4c)	0.89321	0.26074	0.54414		
	$\alpha=\gamma=90$	Li1(4c)	0.17670	0.33424	0.82336		
	$\beta=131.81910$	Li2(4c)	0.13616	0.76511	0.44416		
*C*2 (5)	$a=8.51852$	C1(2b)	0	0.82512	0.5	124.815	−367.5164
monoclinic	$b=3.99771$	O1(4c)	0.76663	0.03642	0.37302	165.873	
Li_4CO_4-**XVIII**	$c=7.84632$	O2(4c)	0.81161	0.61511	0.20056		
	$\alpha=\gamma=90$	Li1(4c)	0.68802	0.55369	0.32375		
	$\beta=152.15270$	Li2(4c)	0.74735	0.10620	0.11248		

© 2007 Wiley-VCH Verlag GmbH & Co. KGaA, Weinheim

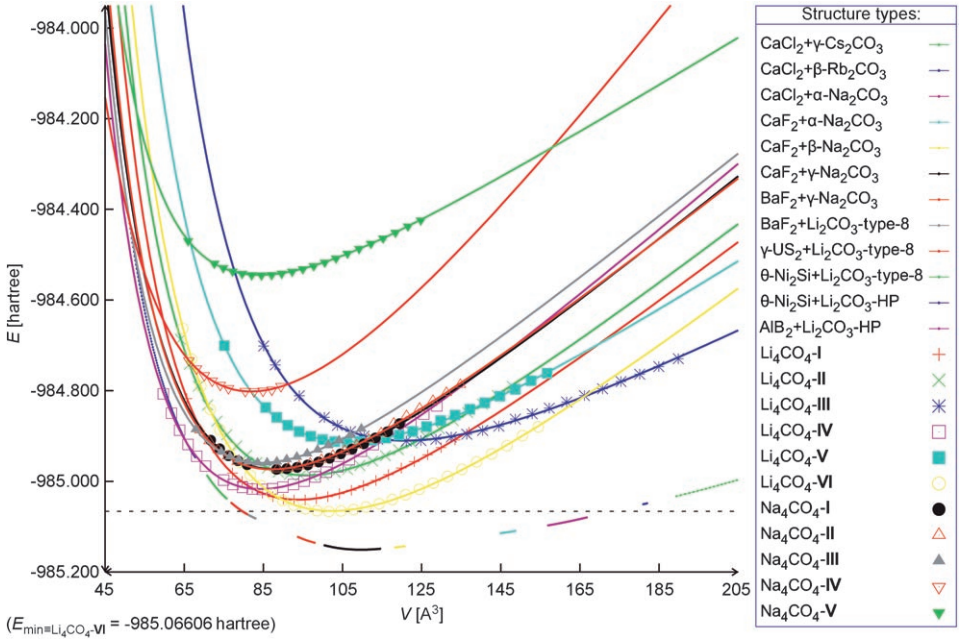

Figure 5. $E(V)$ curves for selected structure candidates calculated on ab initio level (HF) in the Na_4CO_4 system together with the combined curve for $Na_2O+Na_2CO_3$. The dashed horizontal line refers to the energy minimum of the Na_4CO_4 system (E_{min}).

transitions occur in the oxide–carbonate mixture (see Figures 5 and 6), until finally between 37 GPa (DFT-B3LYP) and 60 GPa (HF) a transition to the orthocarbonate phase Li_4CO_4-**IV** take place. As in the case of the Li_4CO_4 system, the DFT-B3LYP calculations show a lower value of the transition pressure than the Hartree–Fock ones. The possible high-pressure structure in the Na_4CO_4 system is shown below (see Figure 15). It appears to belong to the *cP*1 arrangement of heterocubanes (see refs. [25] and [25]). Table 2 and Table S1.2 (Supporting Information) show structural data, minimum volumes, bulk moduli and energies of the selected structure candidates for the Na_4CO_4 system after local optimizations on Hartree–Fock and DFT-B3LYP level.

Table 2. Data for structure candidates for Na_4CO_4 after local optimizations on ab initio level (HF).

Space group (no.) crystal system, type	Lattice constants (a,b,c [Å]; α,β,γ [°])	Atom (multiplicity, Wyckoff letter), relative coordinates				V_{min} [Å^3]	E_{min} [a.u.]
		atom	x	y	z		
$P\bar{4}3m$ (215)	$a=4.54337$	C1(1b)	0.5	0.5	0.5	93.785	−985.0409
cubic	$\alpha=\beta=\gamma=90$	O1(4e)	0.31764	0.31764	0.31764	121.319	
Li_4CO_4-**I**		Na1(4e)	0.78955	0.78955	0.78955		
$R3m$ (160)	$a=4.59298$	C1(1a)	0.99961	0.99961	0.99961	95.754	−984.9874
trigonal	$\alpha=\beta=\gamma=84.77761$	O1(3b)	0.81909	0.81909	0.19316	120.993	
Li_4CO_4-**II**		O2(1a)	0.16322	0.16322	0.16322		
		Na1(1a)	0.71409	0.71409	0.71409		
		Na2(3b)	0.49861	0.49861	0.10286		
$I\bar{4}2m$ (121)	$a=7.74088$	C1(2b)	0	0	0.5	241.899	−984.9108
tetragonal	$c=4.03695$	O1(8i)	0.62481	0.62481	0.79119	86.664	
Li_4CO_4-**III**	$\alpha=\beta=\gamma=90$	Na1(8i)	0.33614	0.33614	0.28782		
$I\bar{4}2m$ (121)	$a=4.37208$	C1(2a)	0	0	0	168.446	−985.0176
tetragonal	$c=8.81221$	O1(8i)	0.79583	0.79583	0.90050	137.398	
Li_4CO_4-**IV**	$\alpha=\beta=\gamma=90$	Na1(8i)	0.69676	0.69676	0.14250		
Cm (8)	$a=7.21635$	C1(2a)	0.00348	0	0.49870	213.095	−984.9128
monoclinic	$b=7.08114$	O1(4b)	0.00048	0.81681	0.69332	105.035	
Li_4CO_4-**V**	$c=4.18698$	O2(2a)	0.81207	0	0.24347		
	$\alpha=\gamma=90$	O3(2a)	0.18915	0	0.35486		
	$\beta=95.13547$	Na1(4b)	0.31427	0.21696	0.00993		
		Na2(4b)	0.20302	0.70794	0.47902		
$C2$ (5)	$a=8.96311$	C1(2a)	0	0.19884	0	204.139	−985.0661
monoclinic	$b=4.97964$	O1(4c)	0.88594	0.03452	0.03816	114.722	
Li_4CO_4-**VI**	$c=4.87118$	O2(4c)	0.08178	0.37127	0.25455		
	$\alpha=\gamma=90$	Na1(4c)	0.26804	0.67518	0.32553		
	$\beta=110.12676$	Na2(4c)	0.11886	0.62838	0.77025		
$R3$ (146)	$a=4.45335$	C1(1a)	0.12305	0.12305	0.12305	88.178	−984.9734
trigonal	$\alpha=\beta=\gamma=88.09780$	O1(3b)	0.98591	0.31795	0.87406	126.426	
Na_4CO_4-**I**		O2(1a)	0.31070	0.31070	0.31070		
		Na1(1a)	0.84400	0.84400	0.84400		
		Na2(3b)	0.33876	0.83598	0.47403		

© 2007 Wiley-VCH Verlag GmbH & Co. KGaA, Weinheim

Table 2. (Continued)

Space group (no.) crystal system, type	Lattice constants (a,b,c [Å]; α,β,γ [°])	Atom (multiplicity, Wyckoff letter), relative coordinates				V_{min} [Å^3]	E_{min} [a.u.]
		atom	x	y	z		
Cm (8)	$a=5.89419$	C1(2a)	0.99963	0	0.43508	174.533	−984.9739
monoclinic	$b=6.62708$	O1(2a)	0.16335	0	0.18105	129.972	
Na_4CO_4-**II**	$c=4.47056$	O2(2a)	0.76084	0	0.30381		
	$\alpha=\gamma=90$	O3(4b)	0.03738	0.18733	0.62191		
	$\beta=91.86530$	Na1(4b)	0.95459	0.72226	0.14556		
		Na2(2a)	0.74955	0	0.79700		
		Na3(2a)	0.34410	0	0.61765		
Cm (8)	$a=6.09363$	C1(2a)	0.89377	0	0.56075	168.898	−984.9592
monoclinic	$b=6.45189$	O1(4b)	0.95928	0.19190	0.76476	133.169	
Na_4CO_4-**III**	$c=4.45444$	O2(2a)	0.02309	0	0.31257		
	$\alpha=\gamma=90$	O3(2a)	0.63709	0	0.41246		
	$\beta=105.32930$	Na1(2a)	0.27477	0	0.77034		
		Na2(2a)	0.69896	0	0.92846		
		Na3(4b)	0.80296	0.71462	0.26562		
*R*3 (146)	$a=4.34481$	C1(1a)	0.62687	0.62687	0.62687	81.849	−984.8018
trigonal	$\alpha=\beta=\gamma=92.10100$	O1(3b)	0.32467	0.52206	0.80594	150.314	
Na_4CO_4-**IV**		O2(1a)	0.85054	0.85054	0.85054		
		Na1(3b)	0.02588	0.79582	0.36314		
		Na2(1a)	0.29818	0.29818	0.29818		
*R*3 (146)	$a=4.40453$	C1(1a)	0.81708	0.81708	0.81708	84.170	−984.5451
trigonal	$\alpha=\beta=\gamma=95.53260$	O1(3b)	0.92787	0.16364	0.63511	106.043	
Na_4CO_4-**V**		O2(1a)	0.54686	0.54686	0.54686		
		Na1(3b)	0.66881	0.41534	0.03897		
		Na2(1a)	0.16853	0.16853	0.16853		

Results restricted to K_4CO_4: Following the same approach as in the cases of Li_4CO_4 and Na_4CO_4 we performed ab initio local optimizations of the K_4CO_4 system. The $E(V)$ curves and structural data are shown in the Figure 7 and Table 3 (for DFT-B3LYP data see Supporting Information, Figure S1.5 and Table S1.3). Again, we found the same general trends with respect to the relation between transition pressure and choice of ab initio method as in the Li_4CO_4 and Na_4CO_4 systems. As we have observed in other systematic exploration of the alkali metal systems (see refs. [10], [11], [27] and [29]), potassium-based compounds exhibit many phase transitions over a comparatively small range of pressures (see e.g. ref. [27]). In these cases, the influence of temperature can affect our ability to predict exactly the sequence of phase transitions. But in the case of the orthocarbonate, the transition pressures are relatively high and the number of competing phases of the oxides and carbonates decreases. According to our calculations, a direct transition from the θ-Ni_2Si modification in the K_2O system plus the γ-Na_2CO_3 modification in the K_2CO_3 system to the K_4CO_4-**III** structure should occur in the range of pressures

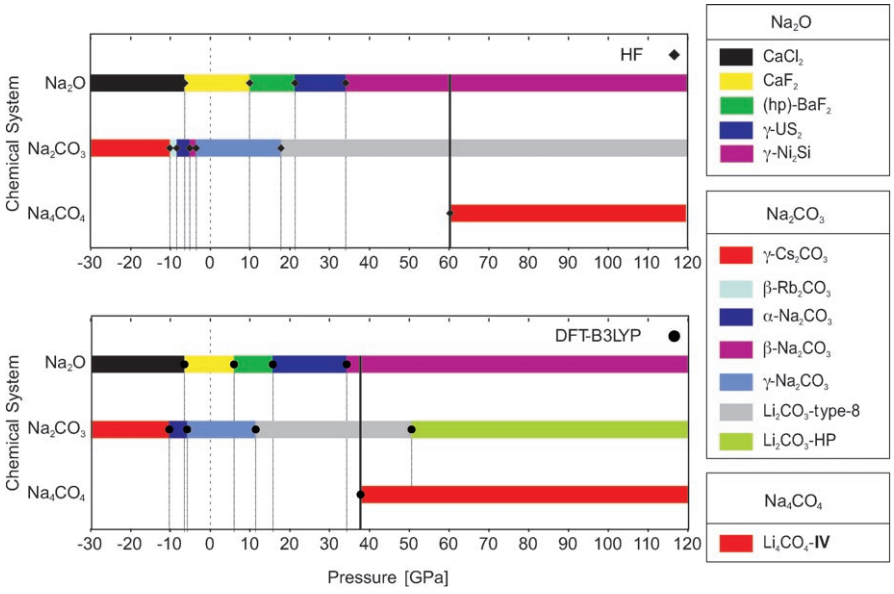

Figure 6. Low-temperature modifications of Na_4CO_4 as function of pressure in equilibrium with the solid state reaction $Na_2O+Na_2CO_3$. Only the modifications with the lowest enthalpy are depicted. Upper box: HF. Lower box: DFT-B3LYP.

© 2007 Wiley-VCH Verlag GmbH & Co. KGaA, Weinheim

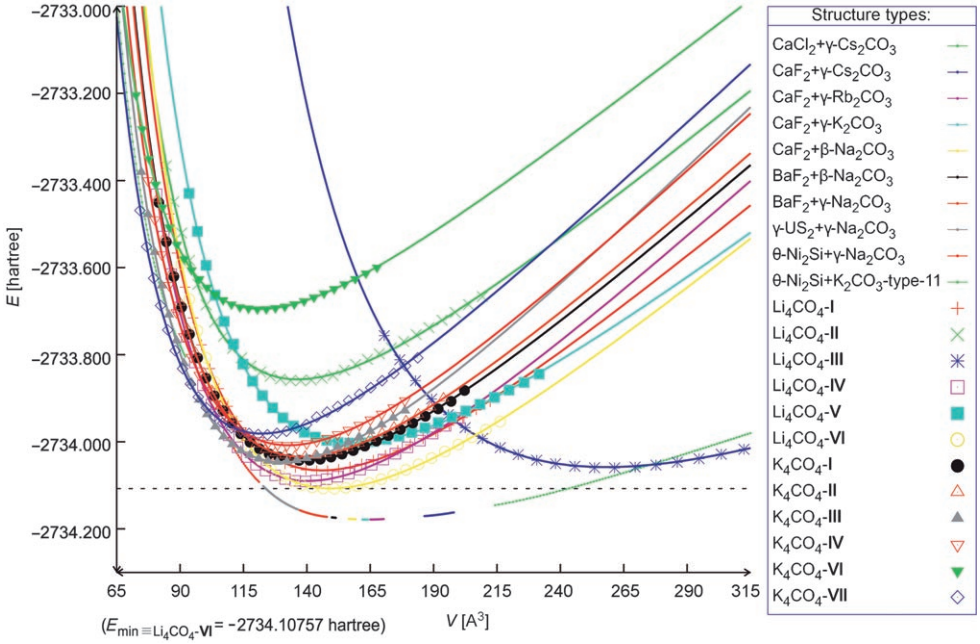

Figure 7. $E(V)$ curves for selected structure candidates calculated on ab initio level (HF) in the K_4CO_4 system together with the combined curve for $K_2O + K_2CO_3$. The dashed horizontal line refers to the energy minimum of the K_4CO_4 system (E_{min}).

Table 3. Data for structure candidates for K_4CO_4 after local optimizations on ab initio level (HF).

Space group (no.) crystal system, type	Lattice constants (a,b,c [Å]; α,β,γ [°])	Atom (multiplicity, Wyckoff letter), relative coordinates				V_{min} [Å^3]	E_{min} [a.u.]
		atom	x	y	z		
$P\bar{4}3m$ (215)	$a=5.25897$	C1(1b)	0.5	0.5	0.5	145.446	−2734.0661
cubic	$\alpha=\beta=\gamma=90$	O1(4e)	0.34189	0.34189	0.34189	82.330	
Li_4CO_4-**I**		K1(4e)	0.79115	0.79115	0.79115		
$R3m$ (160)	$a=5.16252$	C1(1a)	0.99961	0.99961	0.99961	135.974	−2733.8575
trigonal	$\alpha=\beta=\gamma=84.77769$	O1(3b)	0.81909	0.19316	0.81909	87.864	
Li_4CO_4-**II**		O2(1a)	0.16322	0.16322	0.16322		
		K1(1a)	0.71409	0.71409	0.71409		
		K2(3b)	0.49861	0.10286	0.49861		
$I\bar{4}2m$ (121)	$a=9.33983$	C1(2b)	0	0	0.5	515.960	−2734.0592
tetragonal	$c=5.91476$	O1(8i)	0.08625	0.08625	0.36522	41.989	
Li_4CO_4-**III**	$\alpha=\beta=\gamma=90$	K1(8i)	0.84168	0.84168	0.78828		
$I\bar{4}2m$ (121)	$a=5.08784$	C1(2a)	0	0	0	279.911	−2734.0903
tetragonal	$c=10.81314$	O1(8i)	0.83761	0.83761	0.92081	87.477	
Li_4CO_4-**IV**	$\alpha=\beta=\gamma=90$	K1(8i)	0.69365	0.69365	0.14558		
Cm (8)	$a=8.19217$	C1(2a)	0.01715	0	0.55182	316.459	−2734.0028
monoclinic	$b=8.29722$	O1(4b)	0.00205	0.85622	0.70815	74.468	
Li_4CO_4-**V**	$c=4.72962$	O2(2a)	0.89287	0	0.30763		
	$\alpha=\gamma=90$	O3(2a)	0.18803	0	0.48175		
	$\beta=100.14260$	K1(4b)	0.31908	0.18819	0.96024		
		K2(4b)	0.14997	0.69147	0.39179		
$C2$ (5)	$a=10.64862$	C1(2a)	0	0.26132	0	298.154	−2734.1076
monoclinic	$b=5.52021$	O1(4c)	0.91548	0.11545	0.08008	80.546	
Li_4CO_4-**VI**	$c=5.63957$	O2(4c)	0.09037	0.41200	0.21623		
	$\alpha=\gamma=90$	K1(4c)	0.34921	0.52577	0.51073		
	$\beta=115.92290$	K2(4c)	0.13831	0.62488	0.84647		
$R3$ (146)	$a=5.17681$	C1(1a)	0.84605	0.84605	0.84605	138.735	−2734.0430
trigonal	$\alpha=\beta=\gamma=89.95140$	O1(3b)	0.68471	0.97819	0.04222	85.977	
K_4CO_4-**I**		O2(1a)	0.68219	0.68219	0.68219		
		K1(3b)	0.49235	0.13352	0.61950		
		K2(1a)	0.13664	0.13664	0.13664		

 © 2007 Wiley-VCH Verlag GmbH & Co. KGaA, Weinheim

Table 3. (Continued)

Space group (no.) crystal system, type	Lattice constants (a,b,c [Å]; α,β,γ [°])	Atom (multiplicity, Wyckoff letter), relative coordinates				V_{min} [Å^3]	E_{min} [a.u.]
		atom	x	y	z		
Cm (8)	$a=6.83444$	C1(2a)	0.26079	0	0.39829	275.440	−2734.0347
monoclinic	$b=7.33625$	O1(2a)	0.13778	0	0.59975	87.318	
K_4CO_4-**II**	$c=5.54579$	O2(4b)	0.21312	0.16517	0.24823		
	$\alpha=\gamma=90$	O3(2a)	0.47392	0	0.50055		
	$\beta=97.87380$	K1(4b)	0.82275	0.79978	0.67143		
		K2(2a)	0.45915	0	0.01812		
		K3(2a)	0.88905	0	0.20094		
$I\bar{4}$ (82)	$a=6.81932$	C1(2b)	0	0	0.5	259.584	−2734.0465
tetragonal	$c=5.58207$	O1(8 g)	0.03635	0.17543	0.34571	94.405	
K_4CO_4-**III**	$\alpha=\beta=\gamma=90$	K1(8g)	0.90998	0.72416	0.90642		
Cm (8)	$a=6.45640$	C1(2a)	0.02472	0	0.49013	264.731	−2734.0081
monoclinic	$b=7.98047$	O1(4b)	0.47402	0.65297	0.63824	90.538	
K_4CO_4-**IV**	$c=5.19308$	O2(2a)	0.25353	0	0.46844		
	$\alpha=\gamma=90$	O3(2a)	0.89456	0	0.22392		
	$\beta=98.36010$	K1(4b)	0.59838	0.78465	0.23496		
		K2(2a)	0.24363	0	0.96349		
		K3(2a)	0.64390	0	0.71853		
*R*3 (146)	$a=4.95471$	C1(1a)	0.51548	0.51548	0.51548	121.415	−2733.6952
trigonal	$\alpha=\beta=\gamma=87.99350$	O1(3b)	0.59943	0.32848	0.82533	81.922	
K_4CO_4-**VI**		O2(1a)	0.31269	0.31269	0.31269		
		K1(3b)	0.10425	0.31483	0.80713		
		K2(1a)	0.81517	0.81517	0.81517		
$P4_2/n$ (86)	$a=6.66640$	C1(2b)	1/4	1/4	3/4	243.722	−2733.9820
tetragonal	$c=5.48419$	O1(8 g)	0.17621	0.06975	0.58391	96.125	
K_4CO_4-**VII**	$\alpha=\beta=\gamma=90$	K1(8 g)	0.68160	0.45697	0.86563		

between 23 GPa (DFT-B3LYP) and 33 GPa (HF). Upon increasing the pressure we find that the K_4CO_4-**III** modification should exhibit a phase transition to the K_4CO_4-**VII** structure type at 40–45 GPa (cf. Figure 8). Note that in the same range of pressures the carbonate γ-Na_2CO_3 modification undergoes a phase transition to the K_2CO_3-Type-11 modification. The possible high-pressure structures in the K_4CO_4 system are shown below (see Figures 16 and 17). The structures belong to the *tT*2(*II*) (K_4CO_4-**III**) and *oC*2 (K_4CO_4-**VII**) arrangement of heterocubanes (see refs. [25] and [26]). Table 3 and Table S1.3 in the Supporting Information show structural data, minimum volumes, bulk moduli and energies of the selected structure candidates for K_4CO_4 system after local optimizations on Hartree–Fock and DFT-B3LYP level, respectively.

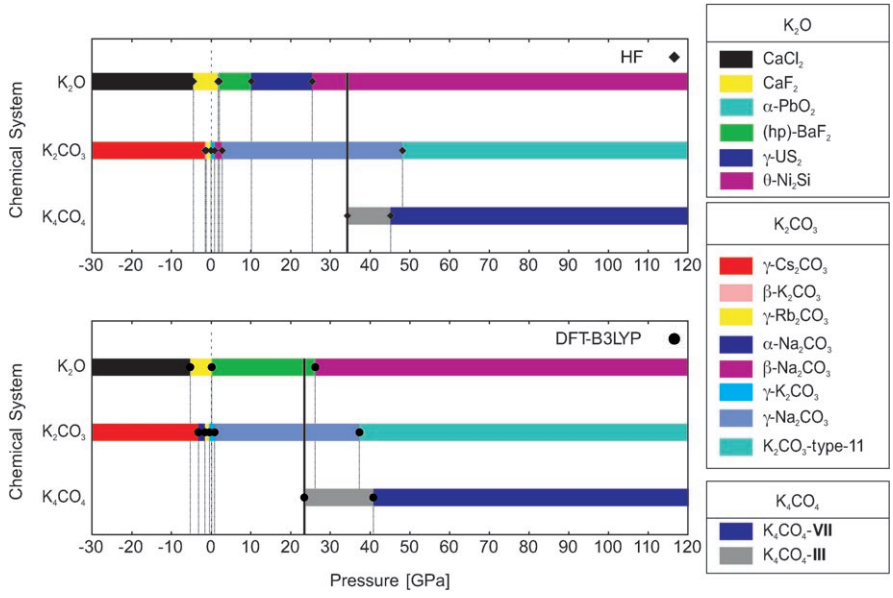

Figure 8. Low-temperature modifications of K_4CO_4 as function of pressure in equilibrium with the solid state reaction $K_2O+K_2CO_3$. Only the modifications with the lowest enthalpy are depicted. Upper box: HF. Lower box: DFT-B3LYP.

Results restricted to Rb_4CO_4: When performing ab initio calculations for Rb_4CO_4, which contains heavy Rb atoms, we encounter potential problems associated with the choice of the basis sets, and, possibly, with relativistic effects. As in the case of Rb_2O and Rb_2CO_3, we have employed the ECP28MBW "Stuttgart/Cologne based"[30] pseudo-potential basis set (PPBS). For the

 © 2007 Wiley-VCH Verlag GmbH & Co. KGaA, Weinheim

Table 4. Data for structure candidates for Rb_4CO_4 after local optimizations on ab initio level (HF).

Space group (no.) crystal system, type	Lattice constants (a,b,c [Å]; α,β,γ [°])	Atom (multiplicity, Wyckoff letter), relative coordinates				V_{min} [Å^3]	E_{min} [a.u.]
		atom	x	y	z		
$P\bar{4}3m$ (215)	$a=5.55848$	C1(1b)	0.5	0.5	0.5	171.739	−432.7075
cubic	$\alpha=\beta=\gamma=90$	O1(4e)	0.34806	0.34806	0.34806	71.744	
Li_4CO_4-**I**		Rb1(4e)	0.78992	0.78992	0.78992		
$R3m$ (160)	$a=6.27378$	C1(1a)	0.99961	0.99961	0.99961	210.809	−432.0655
trigonal	$\alpha=\beta=\gamma=69.98695$	O1(3b)	0.81909	0.19316	0.81909	49.616	
Li_4CO_4-**II**		O2(1a)	0.16322	0.16322	0.16322		
		Rb1(1a)	0.71409	0.71409	0.71409		
		Rb2(3b)	0.49861	0.10286	0.49861		
$I\bar{4}2m$ (121)	$a=8.97453$	C1(2b)	0	0	0.5	436.720	−432.7467
tetragonal	$c=5.42225$	O1(8i)	0.09334	0.09334	0.35101	55.953	
Li_4CO_4-**III**	$\alpha=\beta=\gamma=90$	Rb1(8i)	0.82352	0.82352	0.85641		
$I\bar{4}2m$ (121)	$a=5.35530$	C1(2a)	0	0	0	358.189	−432.7204
tetragonal	$c=12.48952$	O1(8i)	0.84501	0.84501	0.93246	68.888	
Li_4CO_4-**IV**	$\alpha=\beta=\gamma=90$	Rb1(8i)	0.70283	0.70283	0.13724		
Cm (8)	$a=8.65529$	C1(2a)	0.00657	0	0.49656	373.219	−432.2878
monoclinic	$b=8.76626$	O1(4b)	0.99940	0.82590	0.71390	56.408	
Li_4CO_4-**V**	$c=4.99700$	O2(2a)	0.83315	0	0.21440		
	$\alpha=\gamma=90$	O3(2a)	0.19434	0	0.35368		
	$\beta=100.14260$	Rb1(4b)	0.80546	0.69459	0.00932		
		Rb2(4b)	0.69823	0.19818	0.47525		
$C2$ (5)	$a=11.51402$	C1(2a)	0	0.92976	0	379.398	−432.7495
monoclinic	$b=5.98847$	O1(4c)	0.92004	0.06662	0.80202	61.829	
Li_4CO_4-**VI**	$c=6.11798$	O2(4c)	0.07969	0.79521	0.93402		
	$\alpha=\gamma=90$	Rb1(4c)	0.14869	0.69849	0.46219		
	$\beta=115.92290$	Rb2(4c)	0.86013	0.29905	0.11760		
$I\bar{4}2m$ (121)	$a=5.71070$	C1(2b)	0	0	0.5	336.131	−432.7332
tetragonal	$c=10.30694$	O1(8i)	0.35097	0.35097	0.91664	73.537	
Rb_4CO_4-**I**	$\alpha=\beta=\gamma=90$	Rb1(8i)	0.79794	0.79794	0.14703		
Cm (8)	$a=6.74926$	C1(2a)	0.46097	0	0.27718	377.390	−432.7125
monoclinic	$b=9.18786$	O1(4b)	0.90571	0.62834	0.40099	62.756	
Rb_4CO_4-**II**	$c=6.08714$	O2(2a)	0.67300	0	0.24806		
	$\alpha=\gamma=90$	O3(2a)	0.35638	0	0.06563		
	$\beta=91.18920$	Rb1(4b)	0.09280	0.22635	0.07654		
		Rb2(2a)	0.61257	0	0.71980		
		Rb3(2a)	0.05874	0	0.49529		
$R3$ (146)	$a=5.45813$	C1(1a)	0.20172	0.20172	0.20172	162.588	−432.6790
trigonal	$\alpha=\beta=\gamma=90.46120$	O1(3b)	0.32205	0.05017	0.39466	78.548	
Rb_4CO_4-**III**		O2(1a)	0.04315	0.04315	0.04315		
		Rb1(3b)	0.98349	0.50192	0.84502		
		Rb2(1a)	0.49822	0.49822	0.49822		
Cm (8)	$a=6.79048$	C1(2a)	0.96147	0	0.42202	372.618	−432.7133
monoclinic	$b=9.51845$	O1(2a)	0.85319	0	0.19346	63.767	
Rb_4CO_4-**IV**	$c=5.78647$	O2(2a)	0.17173	0	0.39255		
	$\alpha=\gamma=90$	O3(4b)	0.91091	0.87438	0.54675		
	$\beta=94.94170$	Rb1(4b)	0.09914	0.72794	0.22124		
		Rb2(2a)	0.13661	0	0.86776		
		Rb3(2a)	0.56346	0	0.64152		
$I222$ (23)	$a=5.40585$	C1(2c)	0	0	0.5	339.586	−432.7397
orthorhombic	$b=10.50963$	O1(8k)	0.34430	0.58091	0.14104	72.460	
Rb_4CO_4-**VI**	$c=5.97721$	Rb1(8k)	0.82258	0.35170	0.72180		
	$\alpha=\beta=\gamma=90$						
$P\bar{4}$ (81)	$a=6.57331$	C1(1b)	0	0	0.5	137.816	−432.0784
tetragonal	$c=3.18956$	O1(4 h)	0.78245	0.96102	0.82091	85.803	
Rb_4CO_4-**VII**	$\alpha=\beta=\gamma=90$	Rb1(4 h)	0.45965	0.77965	0.26688		
$Amm2$ (38)	$a=7.03882$	C1(2b)	0.5	0	0.59618	283.326	−432.1556
orthorhombic	$b=6.05810$	O1(4e)	0.5	0.25874	0.25090	77.964	
Rb_4CO_4-**VIII**	$c=6.64432$	O2(4c)	0.29329	0	0.44249		
	$\alpha=\beta=\gamma=90$	Rb1(4d)	0	0.74594	0.23866		
		Rb2(4c)	0.71185	0	0.99873		
$P2_1$ (4)	$a=8.80430$	C1(2a)	0.73622	0.27119	0.29928	317.204	−432.7167
monoclinic	$b=5.26961$	O1(2a)	0.64509	0.49302	0.23290	78.758	
Rb_4CO_4-**IX**	$c=6.83880$	O2(2a)	0.65657	0.03345	0.24321		
	$\alpha=\gamma=90$	O3(2a)	0.75563	0.28285	0.51502		

 © 2007 Wiley-VCH Verlag GmbH & Co. KGaA, Weinheim

Table 4. (Continued)

Space group (no.) crystal system, type	Lattice constants (a,b,c [Å]; α,β,γ [°])	Atom (multiplicity, Wyckoff letter), relative coordinates				V_{min} [Å^3]	E_{min} [a.u.]
		atom	x	y	z		
	$\beta = 91.31550$	O4(2a)	0.88695	0.27748	0.20731		
		Rb1(2a)	0.38615	0.76205	0.12444		
		Rb2(2a)	0.42062	0.25194	0.42743		
		Rb3(2a)	0.08862	0.29586	0.58283		
		Rb4(2a)	0.16520	0.26545	0.04059		
Cm (8)	$a = 6.92575$	C1(2a)	0.65347	0	0.27702	321.600	−432.6779
monoclinic	$b = 8.52253$	O1(4b)	0.60124	0.85744	0.40320	76.906	
Rb_4CO_4-**XI**	$c = 5.65858$	O2(2a)	0.87194	0	0.29190		
	$\alpha = \gamma = 90$	O3(2a)	0.54217	0	0.01427		
	$\beta = 103.8027$	Rb1(2a)	0.86224	0	0.76792		
		Rb2(2a)	0.27398	0	0.53325		
		Rb3(4b)	0.25042	0.21097	0.05684		
*C*2 (5)	$a = 12.47167$	C1(2a)	0	0.14944	0	281.089	−432.0778
monoclinic	$b = 3.18265$	O1(4c)	0.87189	0.82302	0.80989	82.205	
Rb_4CO_4-**XII**	$c = 9.04295$	O2(4c)	0.07454	0.47373	0.92464		
	$\alpha = \gamma = 90$	Rb1(4c)	0.33286	0.38468	0.22435		
	$\beta = 128.45410$	Rb2(4c)	0.11936	0.34881	0.44428		

most promising structure types of the Rb_4CO_4 system, $E(V)$ curves and structure data are shown in the Figure 9 and Table 4 (for DFT-B3LYP data see Supporting Information Figure S1.7 and the Table S1.4). Similar to the case of potassium, in the rubidium-based mixture of oxides and carbonates, many phase transitions occur in the pressure range from −5 GPa to +5 GPa. Once again this should not affect our ability to predict high-pressure transitions to the thermodynamically stable orthocarbonate phase. As one can see in Figure 10, in the Rb_4CO_4 system the first transition from Rb_2O (in the γ-US_2 phase) plus Rb_2CO_3 (in the γ-K_2CO_3 phase) to the Rb_4CO_4-**IX** modification should occur between 22 GPa (DFT-B3LYP) and 32 GPa (HF). The Rb_4CO_4-**IX** modification upon increasing pressure transforms into the Rb_4CO_4-**XI** modification between 44 GPa (DFT-B3LYP) and 52 GPa (HF). This time the predicted

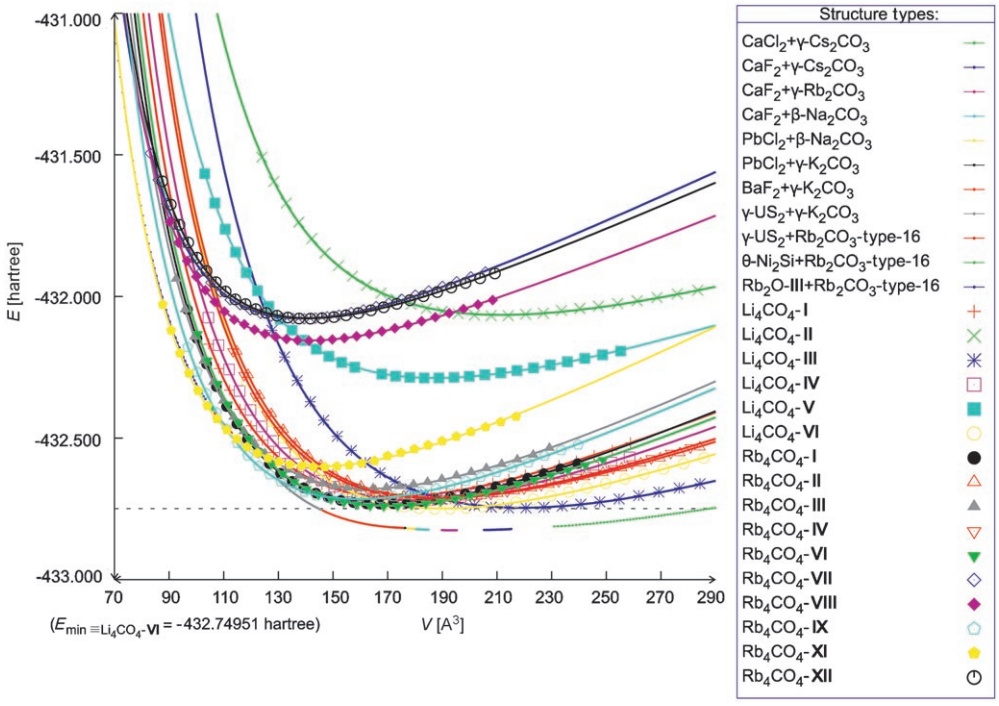

Figure 9. $E(V)$ curves for selected structure candidates calculated on ab initio level (HF) in the Rb_4CO_4 system together with the combined curve for $Rb_2O + Rb_2CO_3$. The dashed horizontal line refers to the energy minimum of the Rb_4CO_4 system (E_{min}).

 © 2007 Wiley-VCH Verlag GmbH & Co. KGaA, Weinheim

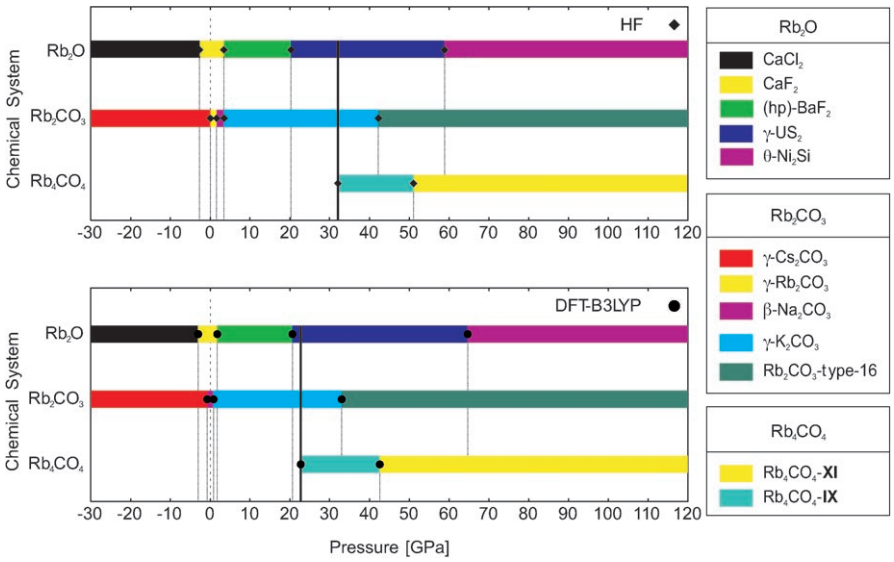

Figure 10. Low-temperature modifications of Rb_4CO_4 as function of pressure in equilibrium with the solid state reaction $Rb_2O + Rb_2CO_3$. Only the modifications with the lowest enthalpy are depicted. Upper box: HF. Lower box: DFT-B3LYP.

structure does not fit into the nomenclature of spatial arrangements of heterocubanes. Table 4 and Table S1.4 in the Supporting Information show structural data, minimum volumes, bulk moduli and energies of the selected structure candidates for Rb_4CO_4 system after local optimizations on Hartree–Fock and DFT-B3LYP level.

Results restricted to Cs_4CO_4: For the same reason as in the case of rubidium, we expect relativistic effects to be possibly of relevance for cesium-based compounds. Thus, we perform all calculations employing an optimized ECP46MWB "Stuttgart/Cologne based" basis set. For the most promising structure types of the Cs_4CO_4 system, $E(V)$ curves and corresponding structure data are shown in Figure 11and Table 5 (for DFT-B3LYP data see Supporting Information Figure S1.9 and Table S1.5). Considering the transition pressures in Figure 12 we find, for both computational procedures (HF and DFT-B3LYP), that in this system the transition to the possible orthocarbonate modification probably will require pressures in excess of 200 GPa. Of course, according to our experience, we cannot fully trust in our calculations in the range of such extremely high pressures, especially if the range must be extrapolated using a fitting formula. We should note that in order to get convergence of the ab initio calculations for several extremely compressed structures under extreme pressures one should perform a re-optimization of the normally frozen basis set for small cell volume, in addition to the regular relaxation of the structure. However, this involves very time-consuming computations, and we can estimate, according to our experi-

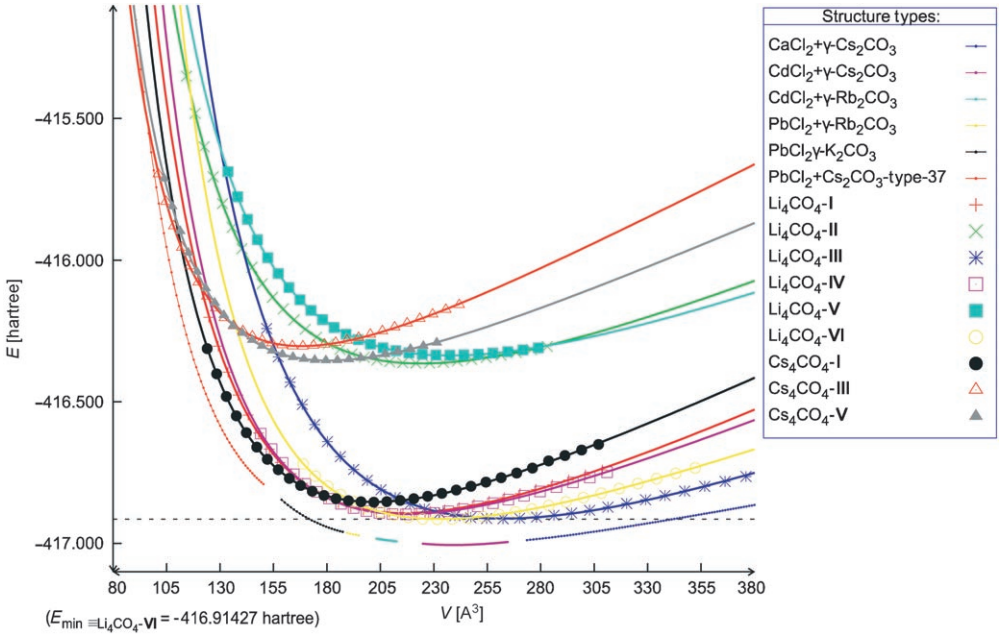

Figure 11. $E(V)$ curves for selected structure candidates calculated on ab initio level (HF) in the Cs_4CO_4 system together with the combined curve for $Cs_2O + Cs_2CO_3$. The dashed horizontal line refers to the energy minimum of the Cs_4CO_4 system (E_{min}).

 © 2007 Wiley-VCH Verlag GmbH & Co. KGaA, Weinheim

Table 5. Data for structure candidates for Cs_4CO_4 after local optimizations on ab initio level (HF).

Space group (no.) crystal system, type	Lattice constants (a,b,c [Å]; α,β,γ [°])	Atom (multiplicity, Wyckoff letter), relative coordinates				V_{min} [Å^3]	E_{min} [a.u.]
		atom	x	y	z		
$P\bar{4}3m$ (215)	$a=5.99260$	C1(1b)	0.5	0.5	0.5	215.201	−416.8931
cubic	$\alpha=\beta=\gamma=90$	O1(4e)	0.35881	0.35881	0.35881	59.526	
Li_4CO_4-**I**		Cs1(4e)	0.78309	0.78309	0.78309		
$R3m$ (160)	$a=6.09349$	C1(1a)	0.99961	0.99961	0.99961	223.599	−416.3640
trigonal	$\alpha=\beta=\gamma=84.77769$	O1(3b)	0.81909	0.19316	0.81909	50.967	
Li_4CO_4-**II**		O2(1a)	0.16322	0.16322	0.16322		
		Cs1(1a)	0.71409	0.71409	0.71409		
		Cs2(3b)	0.49861	0.10286	0.49861		
$I\bar{4}2m$ (121)	$a=9.53209$	C1(2b)	0	0	0.5	523.278	−416.9124
tetragonal	$c=5.75912$	O1(8i)	0.08862	0.08862	0.35686	47.457	
Li_4CO_4-**III**	$\alpha=\beta=\gamma=90$	Cs1(8i)	0.82704	0.82704	0.84449		
$I-42m$ (121)	$a=5.70547$	C1(2a)	0	0	0	433.149	−416.8969
tetragonal	$c=13.30622$	O1(8i)	0.85318	0.85318	0.93648	57.773	
Li_4CO_4-**IV**	$\alpha=\beta=\gamma=90$	Cs1(8i)	0.71283	0.71283	0.13753		
Cm (8)	$a=9.37929$	C1(2a)	0.00657	0	0.49656	474.931	−416.3364
monoclinic	$b=9.49956$	O1(4b)	0.99940	0.82590	0.71390	45.819	
Li_4CO_4-**V**	$c=5.41499$	O2(2a)	0.83315	0	0.21440		
	$\alpha=\gamma=90$	O3(2a)	0.19434	0	0.35368		
	$\beta=100.14260$	Cs1(4b)	0.80546	0.69459	0.00932		
		Cs2(4b)	0.69823	0.19817	0.47525		
$C2$ (5)	$a=12.10943$	C1(2a)	0	0.91735	0	465.675	−416.9143
monoclinic	$b=6.23995$	O1(4c)	0.93850	0.05027	0.82851	51.964	
Li_4CO_4-**VI**	$c=6.36903$	O2(4c)	0.07685	0.78708	0.92336		
	$\alpha=\gamma=90$	Cs1(4c)	0.13463	0.71710	0.42652		
	$\beta=104.62042$	Cs2(4c)	0.85621	0.31113	0.10092		
$R3$ (146)	$a=5.86328$	C1(1a)	0.82954	0.82954	0.82954	201.430	−416.8541
trigonal	$\alpha=\beta=\gamma=88.76340$	O1(1a)	0.97451	0.97451	0.97451	64.026	
Cs_4CO_4-**I**		O2(3b)	0.97729	0.71699	0.65330		
		Cs1(3b)	0.53521	0.04319	0.19094		
		Cs2(1a)	0.53964	0.53964	0.53964		
$C2$ (5)	$a=12.75255$	C1(2b)	0	0.99888	0.5	335.199	−416.3038
monoclinic	$b=3.44604$	O1(4c)	0.57168	0.19662	0.42260	73.627	
Cs_4CO_4-**III**	$c=9.27353$	O2(4c)	0.38126	0.79262	0.32367		
	$\alpha=\gamma=90$	Cs1(4c)	0.38517	0.26635	0.06348		
	$\beta=124.66330$	Cs2(4c)	0.17759	0.24831	0.29000		
$C2$ (5)	$a=13.27106$	C1(4c)	0.20620	0.47656	0.14068	721.164	−416.3543
monoclinic	$b=13.27412$	O1(4c)	0.33002	0.44273	0.98511	59.818	
Cs_4CO_4-**V**	$c=4.09379$	O2(4c)	0.21071	0.47956	0.58343		
	$\alpha=\gamma=90$	O3(4c)	0.61619	0.88139	0.00995		
	$\beta=90.20580$	O4(4c)	0.16997	0.59996	0.98213		
		Cs1(4c)	0.70976	0.27645	0.50761		
		Cs2(2b)	0	0.97318	0.5		
		Cs3(2b)	0	0.29765	0.5		
		Cs4(2a)	0	0.76315	0		
		Cs5(4c)	0.62820	0.64677	0.98582		
		Cs6(2b)	0	0.55229	0.5		

ence, that the reliability of our prediction of transition pressures in this system to be sufficiently high at least up to 150 GPa. We further note that our calculated transition pressures in the range of 220 to 310 GPa are probably the upper limit of the transition pressure in Cs_4CO_4 system. We can roughly estimate that the actual pressure in the case of Cs_4CO_4 could be up to 50 GPa lower than those predicted by our calculations using frozen basis sets. As in the case of Rb_4CO_4 the predicted structure of the Cs_4CO_4 does not fit into the nomenclature of spatial arrangements of heterocubanes. Table 5 and Table S1.5 in the Supporting Information show structural data, minimum volumes, bulk moduli and energies of the selected structure candidates for Cs_4CO_4 system after local optimizations on Hartree–Fock and DFT-B3LYP level.

Discussion

In this work we have presented structure candidates for the alkali metal orthocarbonates at low temperatures and pressures up to 250 GPa. We have computed transition pressures for the solid state reaction $A_2O + A_2CO_3 \rightleftarrows A_4CO_4$ (A = Li, Na, K, Rb, and Cs). The results of the calculations show

 © 2007 Wiley-VCH Verlag GmbH & Co. KGaA, Weinheim

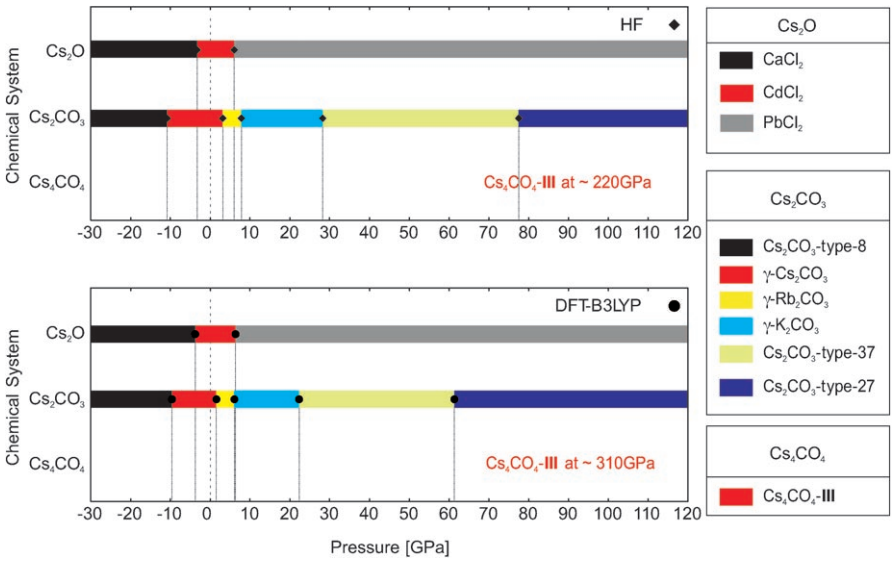

Figure 12. Low-temperature modifications of Cs_4CO_4 as function of pressure in equilibrium with the solid state reaction $Cs_2O + Cs_2CO_3$. Only the modifications with the lowest enthalpy are depicted. Upper box: HF. Lower box: DFT-B3LYP.

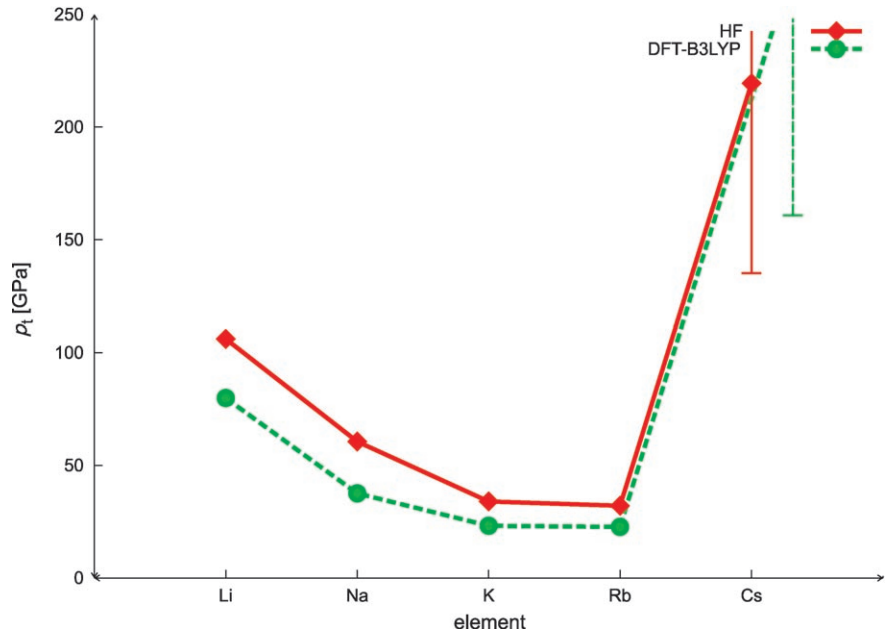

Figure 13. Transition pressures between the mixture A_2O + A_2CO_3 and the orthocarbonate A_4CO_4.

that, at zero temperature and zero pressure, there exists only the mixture of the corresponding most stable modifications in the system A_2O and A_2CO_3. We find that potassium and rubidium show relatively low transition pressures from A_2O-plus-A_2CO_3 to the hypothetical modifications of A_4CO_4. Considering the cation size, one would expect the lithium orthocarbonate to have the lowest pressure of formation, while when arguing from alkali oxide basicity, cesium orthocarbonate should appear first as function of pressure. Actually the opposite trend has been found: plotting the cations versus transition pressure to the hypothetical modifications in the A_4CO_4 system we find a minimum for K and Rb (see Figure 13).

In order to gain some estimate for the uncertainty in the theoretical results we have employed two different Hamiltonians (HF and DFT) while using the same combinations of slightly re-optimized basis sets for all three classes of systems: oxides, carbonates and orthocarbonates. As we have discussed in reference [10,11] and [29], essentially all volumes calculated with HF are somewhat larger than the experimental ones, and cells computed with DFT-B3LYP are close to or smaller than experimental values, respectively. This fits our general observation in all of the system we have studied. This also suggests that the experimental transition pressure should lie between the ones calculated with HF (upper limit) and DFT (lower limit).

As we commented in an earlier paper,[27] within a given group of ab initio methods (HF and DFT) there exists sometimes a noticeable dependence on the choice of basis sets. For this reason we have performed some additional optimizations of the outermost coefficients of the basis sets[2] in a few cases. In order to avoid the problem of basis set comparability while studying rather different systems with the same overall composition A_4CO_4 and A_2O plus A_2CO_3, basis sets employed in calculations of the orthocarbonates are almost the same as the ones for the oxides and carbonates.

We should note that we cannot guarantee that our global search procedure will identify all possible candidates for high-pressure structures. Considering the complexity of the

[2] The main basis set optimization task had been performed during earlier studies in other systems. For example, optimizations and testing of the alkali metal basis sets was mostly accomplished in the system of alkali metal sulfides (see ref. [27]). Then, fine tuning of the alkali metal basis sets and optimization of the oxygen basis set has been performed in the alkali metal oxides (see ref. [11]). Finally, the main optimization of the carbon basis set has been done in the alkali metal carbonates (see ref. [10]).

 © 2007 Wiley-VCH Verlag GmbH & Co. KGaA, Weinheim

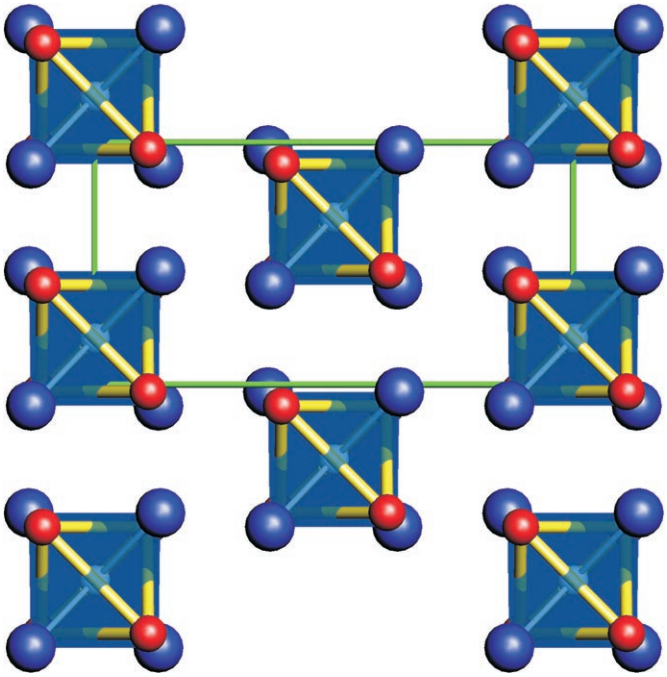

Figure 14. High-pressure modification of Li_4CO_4 system: Li_4CO_4-**X**. Little (red) spheres refer to oxygen, big (blue) spheres refer to the alkali metal (A = Li, Na, K, Rb, Cs), and little (white) spheres in the center of the oxygen tetrahedra refer to carbon.

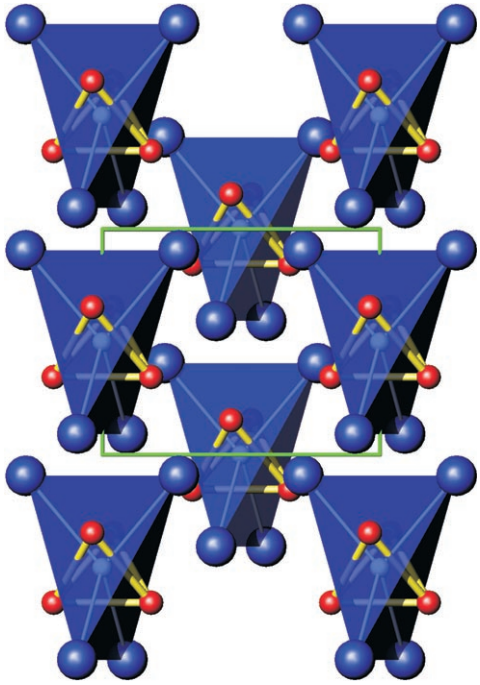

Figure 16. High-pressure modification of K_4CO_4 system: K_4CO_4-**III**. For notation see Figure 14.

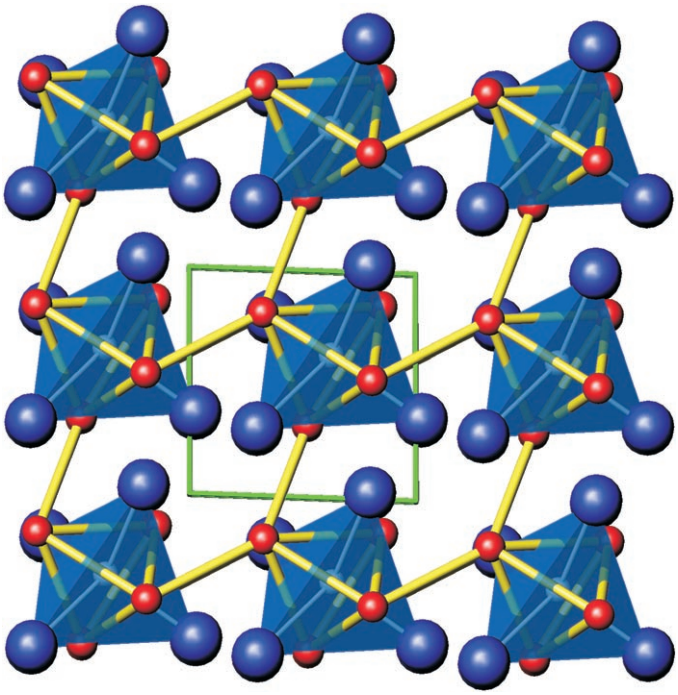

Figure 15. High-pressure modification of Na_4CO_4 system: Na_4CO_4-**IV**. For notation see Figure 14.

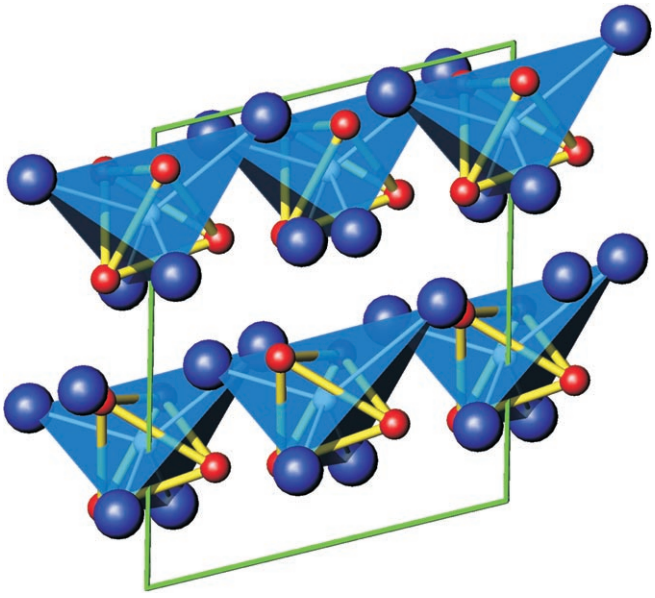

Figure 17. High-pressure modification of K_4CO_4 system: K_4CO_4-**VII**. For notation see Figure 14.

landscapes, missing a relevant candidate is most likely to happen for the orthocarbonates and less likely so for the oxides and carbonates, in particular since already employing three formula units during the global optimization of the orthocarbonates proved to be computationally very expensive. However, if another thermodynamically more stable candidate existed among the orthocarbonates, then this would actually result in a lower transition pressure. Thus, we suggest that our predicted pressures are most likely upper limits for

 © 2007 Wiley-VCH Verlag GmbH & Co. KGaA, Weinheim

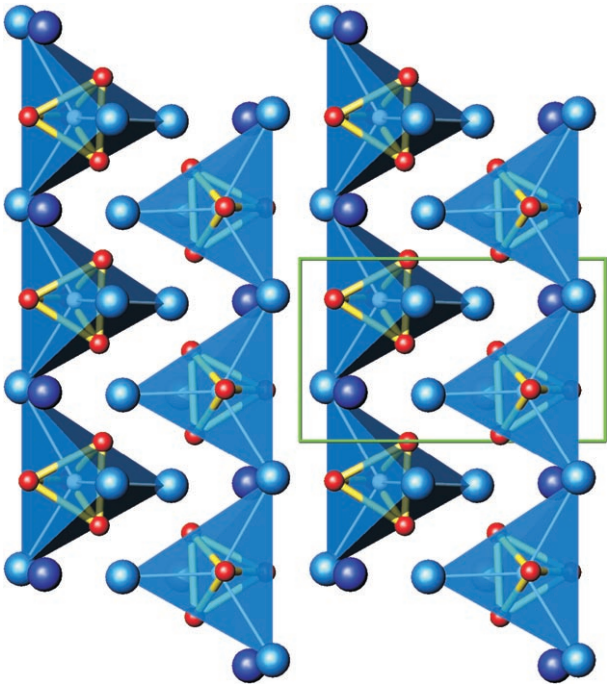

Figure 18. High-pressure modification of Rb_4CO_4 system: Rb_4CO_4-**IX**. For notation see Figure 14.

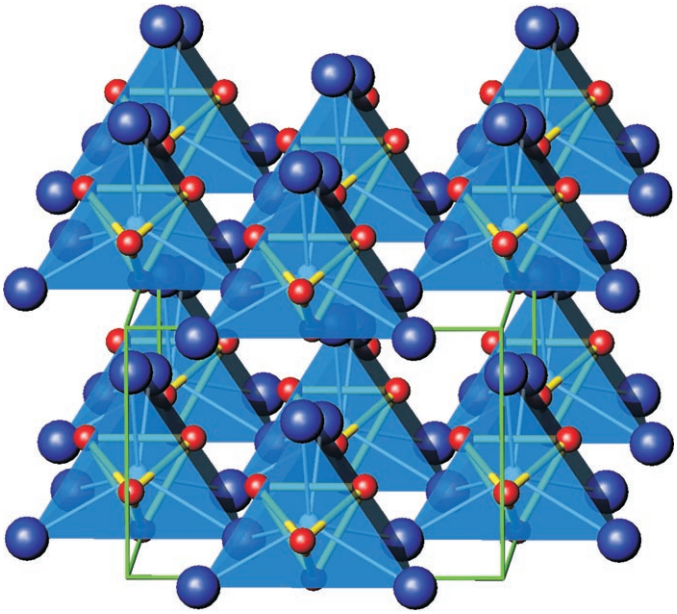

Figure 19. High-pressure modification of Rb_4CO_4 system: Rb_4CO_4-**XI**. For notation see Figure 14.

the actual transition pressures (even though this would regrettably imply that we would not have found the correct modification!).

Finally, there is the surprisingly high expected transition pressure for Cs_4CO_4. Possible sources of error associated with the ab initio calculation of Cs_4CO_4 are relativistic effects and dispersive interactions, which are of particular importance for Cs, and which can only be partly accounted for in the choice of basis sets and pseudopotentials. Furthermore, experience has shown that the extrapolation of the fit of the $E(V)$ curve with the Murnaghan formula can be very sensitive to the number of calculated data points, in particular for very small volumes and high pressures. Finally, a possible reason might be the relatively large size of the cesium atoms, which do not allow sufficiently regular joint packing of the CO_4 units and the Cs atoms, and thus forces the system into energetically unfavorable arrangements compared to the ones exhibited by for example, K_4CO_4 or Rb_4CO_4.

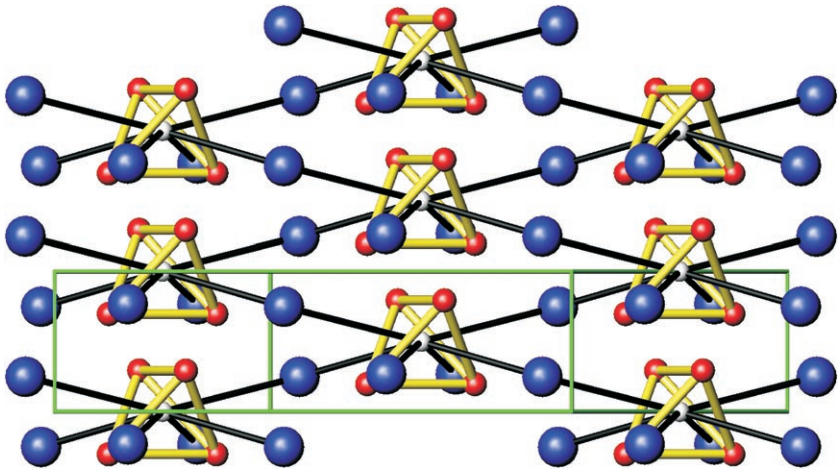

Figure 20. High-pressure modification of Cs_4CO_4 system: Cs_4CO_4-**III**. For notation see Figure 14.

Acknowledgement

Funding was provided by the BMBF via grant No. 03C0352. We would like to thank J. Nuss for many valuable discussions.

[1] M. Al-Shemali, A. I. Boldyrev, *J. Phys. Chem. A* **2002**, *106*, 8951.
[2] A. E. Reed, C. Schade, P. von Ragué Schleyer, P. V. Kamath, J. Chandrasekhar, *J. Chem. Soc. Chem. Commun.* **1988**, 67.
[3] N. Narasimhamurthy, H. Manohar, A. G. Samuelson, J. Chandrasekhar, *J. Am. Chem. Soc.* **1990**, *112*, 2937.
[4] C. Mellot-Draznieks, S. Girard, G. Ferey, Ž. Čančarević, J. C. Schön, M. Jansen, *Chem. Eur. J.* **2002**, *8*, 4102.
[5] J. Arlt, M. Jansen, *Chem. Ber.* **1990**, *124*, 321.

 © 2007 Wiley-VCH Verlag GmbH & Co. KGaA, Weinheim

[6] M. Jansen, *Angew. Chem.* **1979**, *91*, 762; *Angew. Chem. Int. Ed. Engl.* **1979**, *18*, 698.
[7] T. Bremm, M. Jansen, *Z. Anorg. Allg. Chem.* **1992**, *608*, 49.
[8] A. Neuhaus, *Chimia* **1964**, *18*, 93.
[9] A. R. Oganov, C. W. Glass, S. Ono, *Earth Planet. Sci. Lett.* **2006**, *241*, 95.
[10] Ž. Čančarević, J. C. Schön, M. Jansen, *Z. Anorg. Allg. Chem.* **2006**, *632*, 1437.
[11] Ž. Čančarević, J. C. Schön, M. Jansen, *Phys. Rev. B* **2006**, *73*, 224114.
[12] J. C. Schön, M. Jansen, *Angew. Chem.* **1996**, *108*, 1358; *Angew. Chem. Int. Ed. Engl.* **1996**, *35*, 1286.
[13] M. Jansen, *Angew. Chem.* **2002**, *114*, 3896; *Angew. Chem. Int. Ed.* **2002**, *41*, 3747.
[14] J. C. Schön, M. Jansen, *Z. Kristallogr.* **2001**, *216*, 307–325; J. C. Schön, M. Jansen, *Z. Kristallogr.* **2001**, *216*, 361–383.
[15] J. Emsley, *The Elements*, Clarendon Press, Oxford, **1992**.
[16] W. Ostwald, *Z. Phys. Chem. (Leipzig)* **1897**, *22*, 282.
[17] D. Fischer, Ž. Čančarević, J. C. Schön, M. Jansen, *Z. Allgem. Anorg. Chem.* **2004**, *630*, 156.
[18] S. Kirkpatrick, C. D. Gelatt Jr. , M. P. Vecchi, *Science* **1983**, *220*, 671.
[19] V. Czerny, *J. Optim. Theo. Appl.* **1985**, *45*, 41.
[20] http://www.crystal.unito.it/Basis Sets/Ptable.html, **2006**.
[21] http://www.theochem.uni-stuttgart.de/, **2006**.
[22] F. D. Murnaghan, *Proc. Natl. Acad. Sci. USA* **1944**, *30*, 244.
[23] J. C. Schön, *Ber. Bunsenges.* **1996**, *100*, 1388.
[24] J. C. Schön, H. Putz, M. Jansen, *J. Phys. Condens. Matter* **1996**, *8*, 143.
[25] J. Nuss, PhD Thesis, University of Osnabrueck, Osnabrueck (Germany), **1995**.
[26] H. G. von Schnering, R. Nesper, *Z. Kristallogr.* **1983**, *162*, 202.
[27] J. C. Schön, Ž. Čančarević, M. Jansen, *J. Chem. Phys.* **2004**, *121*, 2289.
[28] A. Grezchnik, P. Bouvier, L. Farina, *J. Solid State Chem.* **2003**, *173*, 13.
[29] Ž. Čančarević, PhD Thesis, University of Stuttgart, Stuttgart (Germany), **2006**.
[30] "Library keywords are of the form ECPnXY; n is the Number of core electrons which are replaced by the pseudopotential, X denotes the reference system used for generating the pseudopotential (X = S: single-valence-electron ion; X = M: neutral atom), and Y stands for the theoretical level of the reference data (Y = HF: Hartree-Fock; Y = WB: quasi-relativistic; Y = DF: relativistic). For one- or two-valence electron atoms SDF is a good choice, while otherwise MWB or MDF is recommended. (For light atoms, or for the discussion of relativistic effects, the corresponding SHF, MHF pseudopotentials may be useful.) The same keyword applies to the set of pseudopotential parameters and the corresponding optimized valence basis sets." (http://iris.theochem.unistuttgart.de/pseudopotentials/), **2006**.

Received: November 15, 2006
Published online: June 21, 2007

 © 2007 Wiley-VCH Verlag GmbH & Co. KGaA, Weinheim